DIAMOND OXIDATION EXPERIMENTS IN Cl^--H_2O FLUIDS: IMPLICATIONS FOR KIMBERLITIC AND MANTLE FLUID COMPOSITIONS, AND DIAMOND OXIDATION MECHANISMS

Luke Hilchie

Submitted in Partial Fulfillment of the Requirements
for the Degree of Bachelor of Sciences, Honours
Department of Earth Sciences
Dalhousie University, Halifax, Nova Scotia
March 16, 2009

DALHOUSIE UNIVERSITY
Inspiring Minds

Department of Earth Sciences
Halifax, Nova Scotia
Canada B3H 4J1
(902) 494-2358
FAX (902) 494-6889

DATE: Apr. 23/2009

AUTHOR: Luke Hilchie

TITLE: Diamond oxidation experiments in Cl-H_2O fluids: Implications for kimberlitic and mantle fluid compositions, and diamond oxidation mechanisms

Degree: BSc Honours Convocation: May Year: 2009

Permission is herewith granted to Dalhousie University to circulate and to have copied for non-commercial purposes, at its discretion, the above title upon the request of individuals or institutions.

Signature of Author

Abstract

Diamond dissolution experiments in Cl^--H_2O fluids produce distinctive resorption features on diamonds and reveal insights into diamond oxidation mechanisms, with implications for kimberlitic and mantle fluids. Experiments at 1350 °C and 1 GPa show that chloride-rich aqueous fluids produce few edge dissolution features and abundant trigons on octahedron faces. Deep etch channels form within some trigons. These features occur naturally and have not previously been produced experimentally, implying that natural diamonds with etch channels may have been dissolved in chloride-rich fluid. The formation of etch channels within trigons supports a defect-related origin of these features. Reduction of edge dissolution in chloride-rich aqueous fluid may result from cations blocking electron-dense diamond edges and vertices, preventing polar water molecules from preferentially dissolving these sites. This interpretation provides an explanation for previously observed face-dominated dissolution features produced in CO_2 fluid. Future experiments will explore diamond dissolution in Cl^--CO_2 fluids and the effect of other polar and non-polar solvents on diamond dissolution features. Comparison of experimental results to natural diamonds may elucidate the importance of chloride in kimberlitic or mantle fluids.

Key Words: diamond oxidation, diamond dissolution, primary kimberlite fluid composition, Udachnaya-East, chlorides, mantle fluids, experimental petrology

TABLE OF CONTENTS

Abstract i

List of figures iii

List of tables iv

Acknowledgements v

Chapter 1: Introduction 1

1.1 Kimberlites 1
1.1.1 General background 1
1.1.2 Kimberlite composition 4
1.2 Diamonds 7
1.2.1 Diamond surface features 8
1.2.2 Mechanism of diamond oxidation 11
1.3 Investigating chloride in kimberlites using diamond surface features 12

Chapter 2: Materials and methods 14

2.1 Overview 14
2.2 Sample selection and preparation 15
2.3 Reagents and starting compositions 15
2.4 101 kPa experiments 16
2.5 1 GPa experiments 17
2.5.1 Apparatus' structure and function 17
2.5.2 Pressure correction 19
2.5.3 Sample preparation and setup 20
2.5.4 Procedure 20
2.6 Scanning electron microscopy 21

Chapter 3: Results 22

3.1 Diamond dissolution experiments in NaCl and Air at 101 kPa, 885 °C 22
3.2 Diamond dissolution experiments in H_2O-Cl^- at 1 GPa, 1350 °C 22
3.2.1 Diamond surface features produced in H_2O fluid 22
3.2.2 Diamond surface features produced in NaCl-H_2O fluids 26
3.2.3 Diamond surface features produced in KCl-H_2O fluids 34
3.2.4 Comparison of diamond dissolution features produced by NaCl-H_2O and KCl-H_2O fluids 40
3.2.5 Platinum mobilization in Cl^--H_2O fluids 44

Chapter 4: Discussion 47

4.1 Diamond oxidation mechanisms in Cl^--H_2O systems 47
4.1.1 Molten chloride-diamond interactions 47
4.1.2 The role of defect in determining etch pit sites 50
4.1.3 Electrostatic interactions in diamond oxidation 51
4.2 Use of diamond surface features as records of chloride content in diamond dissolving fluids 53
4.2.1 Distinctive diamond surface features produced by Cl^--H_2O fluids 53
4.2.2 Interpreting natural diamond populations 55

Chapter 5: Conclusions 58

5.1 Chloride-rich aqueous fluid produces distinctive dissolution features on diamond surfaces 58
5.1.1 Diamond surface features: a proxy for chloride content in diamond-dissolving fluids? 59
5.2 Mechanisms of diamond oxidation 60
5.2.1 The role of electrostatic attraction in diamond oxidation 60
5.2.2 The role of crystal defects in determining etch pit sites 60

References 62

LIST OF FIGURES

Figure 1.1: Generalized model of a kimberlite pipe, showing root, diatreme and crater zones.....3

Figure 1.2: Morphological progression of a diamond octahedron with increasing dissolution.....7

Figure 1.3: Octahedral diamonds typically display triangular etch pits (trigons) produced during dissolution
Figure 2.1: Ternary plot of molar fluid compositions studied in 1 GPa experiments.....14

Figure 2.2: Experimental setup for 101 kPa experiments.....17

Figure 2.3: Pressure plate of the piston-cylinder (a) and cell assembly (b) used in 1 GPa experiments 18

Figure 3.1: Diamond surface features produced in molten NaCl and air at 885 °C and 101 kPa 25

Figure 3.2: Representative images of diamond surface before (a) and after (b, c, d) exposure to H_2O fluid for 60 minutes at 1350 °C and 1 GPa.....26

Figure 3.3: General view of diamond surfaces before and after exposure to NaCl-H_2O fluids for 60 minutes at 1350 °C and 1 GPa.....27

Figure 3.4: Diamond surface after exposure to 5% NaCl aqueous fluid for 60 minutes at 1350 °C and 1 GPa.....29

Figure 3.5: Diamond surface after dissolution in 30% NaCl aqueous fluid for 60 minutes at 1350 °C and 1 GPa.....30

Figure 3.6: Diamond surface after dissolution in 60% NaCl aqueous fluid for 60 minutes at 1350 °C and 1 GPa.....32

Figure 3.7: Diamond surfaces after dissolution in NaCl melt for 60 minutes at 1350 °C and 1 GPa.....33

Figure 3.8: General view of diamond surfaces before and after exposure to KCl-H_2O fluids 35

Figure 3.9: Oxidation by 30% KCl-70% H_2O fluid produces step faces, hillocks on diamond edges and large trigons on faces.....37

Figure 3.10: Diamond surface after dissolution in 60% KCl aqueous fluid for 60 minutes at 1350 °C and 1 GPa.....38

Figure 3.11: Diamond surface after dissolution in KCl melt for 56 minutes at 1350 °C and 1 GPa.....39

Figure 3.12: Comparison between dissolution features produced in 30% NaCl and KCl aqueous fluid 42

Figure 3.13: Comparison between diamond dissolution features produced by 60% NaCl and KCl aqueous fluids.....43

Figure 3.14: Comparison between dissolution features produced in molten NaCl and KCl 45

Figure 3.15: Platinum (Pt) spheroids on diamond surfaces after dissolution in 30% and 60% NaCl aqueous fluids and molten KCl 46

Figure 4.1: Generic liquid immiscibility curve for a binary system (components A and B) at constant pressure 48

Figure 4.2: Cartoon schematic illustrating the potential role of electrostatic interactions in diamond dissolution 52

LIST OF TABLES

Table 3.1: Summary of conditions for all experiments. All samples were partially dissolved during experiment.....23

Table 3.2: Summary of dissolution features produced on diamond during 1 GPa experiments 24

ACKNOWLEDGEMENTS

This work was made possible by financial support from the Natural Sciences and Engineering Research Council of Canada and diamonds provided generously by BHP Billiton Diamonds Incorporated. More personally, I gladly thank Yana Fedortchouk for her patience, guidance and remarkable availability during this work. I thank the other students who undertook this responsibility, in particular my fellow experimenter Liz McIsaac for always letting me bounce ideas off her. I thank Patricia Scallion for her assistance with the scanning electron microscope, and Dan MacDonald for expedient carbon-coating. Although not involved in this project, I thank Rebecca Jamieson for introducing me to research. I thank my parents, brothers and sisters-in-law and my nephews for their support over many years. I am truly indebted to my wife, Ashley, who has listened to every thought and supported me for each day of this project and degree.

CHAPTER 1: INTRODUCTION

1.1 Kimberlites

1.1.1 General background

Kimberlites are exotic volcanic rocks derived from *ca.* 200 km depth beneath continents. The name originates from the town of Kimberley, South Africa, where kimberlites were first discovered and described. Kimberlites typically occur within stable Precambrian cratons, usually forming carrot-shaped structures called pipes. Kimberlite magma entrains and transports foreign materials from the mantle and crust to the Earth's surface. Such materials include rocks fragments (xenoliths) and individual minerals (xenocrysts). The most economically important material transported by kimberlite is diamond, which is present in only a small proportion of kimberlites (Mitchell, 1996).

Kimberlites are categorized as Group I or Group II on the basis of mineralogy. Group I kimberlites characteristically feature a macrocryst assemblage consisting of xenocrysts and phenocrysts. Olivine is always present and is the most common macrocryst, while garnet, Mg-ilmenite, Cr-diopside and chromite are also common. Commonly occurring groundmass minerals include olivine, monticellite, perovskite (rare Earth element- and Sr-poor), calcite, dolomite and serpentine. Group I kimberlites are consequently ultramafic (silica-poor), magnesian and CO_2-rich. Group II kimberlites (orangeites) do not typically contain a macrocryst assemblage, and usually have abundant phlogopite. They feature a variety of minerals that are absent or rare in Group I kimberlites, including a wide array of exotic carbonates, rare Earth element- and Sr-rich perovskite, barite, Mn-ilmenite and leucite. Orangeites lack some typical Group I kimberlite minerals, such as monticellite and chromite, and usually have much less

olivine. Despite these and other distinguishing mineralogical features, it can be difficult to distinguish the two groups, as both types of kimberlites can be very heterogeneous and highly altered rocks. Specific minerals' compositions, such as perovskite and phlogopite, can also be used to differentiate between the two groups. Group I and II kimberlites are not genetically related, and are often discussed separately in the literature (Mitchell, 1996). The term kimberlite usually refers to Group I kimberlites when not otherwise specified. This convention is adopted here because this investigation is concerned only with Group I kimberlites. Kimberlites are subdivided based on textural characteristics into coherent kimberlite and volcaniclastic kimberlite. Coherent kimberlite is kimberlite that has not been fragmented during eruption. Volcaniclastic kimberlite consists of all kimberlite material that has been disaggregated from its coherent state, and includes pyroclastic and resedimented subdivisions. Scott-Smith *et al* (2008) provide detailed instructions on the current state of kimberlite classification. The reader should note that kimberlite classification is a rigorous process and more details must be considered than are presented above.

Although kimberlite eruption has never been directly observed, models of kimberlite emplacement have been assembled from geological evidence, such as structure, lithology, mineralogy and petrographic texture. Kimberlite pipes are traditionally divided into three zones based on their structure and lithology: root, diatreme and crater zones (Fig. 1.1). Each has a predominant facies: hypabyssal, diatreme and crater facies. The root zone consists of magmatic kimberlite not associated with a free fluid phase. It forms tabular intrusive structures (dykes and sills). As magmatic kimberlite ascends, fluid exsolution or contamination introduces a free fluid

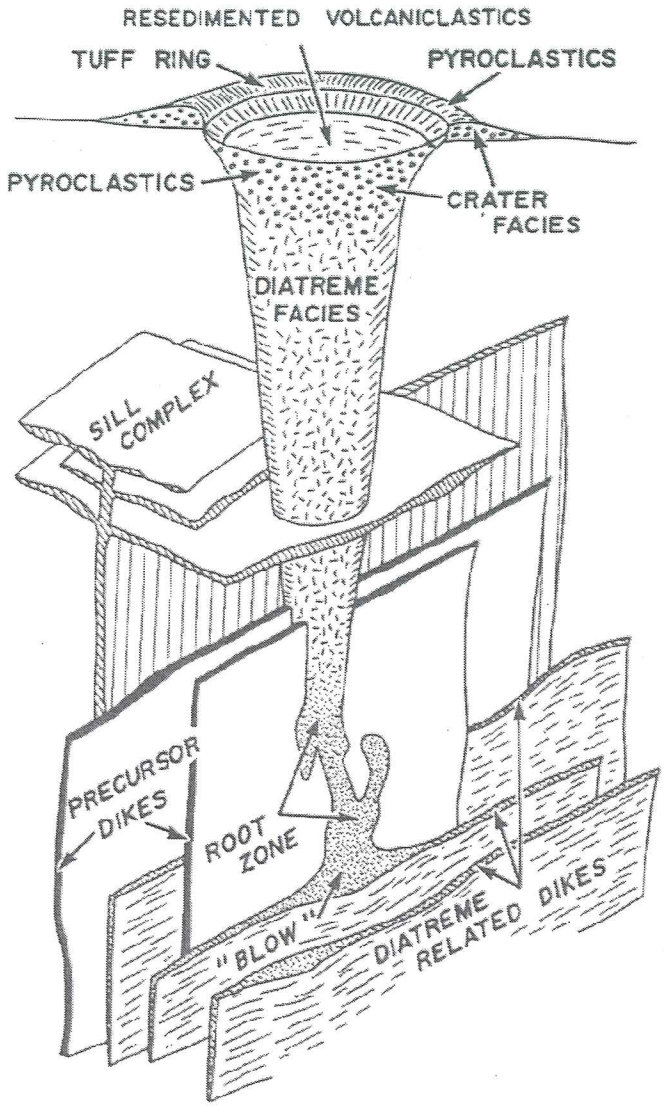

Figure 1.1: Generalized model of a kimberlite pipe, showing root, diatreme and crater zones. Not to scale. From Mitchell (1986).

phase which dramatically changes the kimberlite's mechanical properties. The diatreme facies kimberlite represents fluid-rich, rapidly ascending kimberlite material. This facies forms the carrot-shaped structure. Explosive eruption near the surface produces a crater by ejecting kimberlite material into the air, which is returned to the crater by direct in-fall of ejected material or later resedimentation by surface runoff waters (Scott-Smith, 1996).

Kimberlite mineralogy is complex, as discussed above, and is a result of the different processes involved in kimberlite formation. The minerals are often grouped by size into the macrocryst and groundmass suites. Macrocryst minerals represent both phenocrysts derived from kimberlite magma and foreign minerals disaggregated from their host rock. They can include olivine, garnet, Cr-diopside, Mg-ilmenite and chromite among others. Groundmass minerals mainly represent later-crystallized kimberlite magma. They include olivine, carbonates, monticellite, phlogopite, perovskite and many minerals. Both suites can be infiltrated by deuteric fluids, producing serpentine and carbonates as a result of low-temperature alteration reactions. It is frequently difficult to distinguish endogenous minerals from exogenous material, or alteration mineralogy from primary mineralogy, because their chemical compositions are often not distinctive (Scott-Smith, 1996). Mitchell (2008) argued that the alteration processes affecting kimberlites are part of the kimberlite system itself, as opposed to unrelated secondary processes.

1.1.2 Kimberlite composition

Primary composition of an igneous system refers to the original magma composition prior to volatile extraction or post-magmatic alteration. In contrast, parental composition is the original melt composition melted from the source, prior to such primary processes as crystal fractionation and assimilation. Parental and primary melt compositions are fundamental parameters of any igneous system, and are central to interpreting the origins and significance of an igneous body. In general, geochemical analyses of kimberlite show that kimberlites have fairly consistent composition in time and space, implying that a similar magma source has underlain all continents for more than 1 Ga. Hence, understanding primary kimberlite composition has major significance

for understanding this important source rock. However, parental and primary kimberlite compositions remain unknown due to contamination and assimilation, post-magmatic alteration and volatile loss associated with eruption (Scott-Smith, 1996). Because of these reasons geochemical analyses of apparently unaltered, undifferentiated kimberlite likely do not represent true primary compositions. In general, kimberlites are considered to be ultramafic (*i.e.*, silica-poor), magnesian and alkaline rocks, as these characteristics are common to most kimberlites. Increasing evidence suggests that there is a carbonatitic component present in primary kimberlite (Francis and Patterson, 2009).

It is well-agreed that kimberlite must be volatile-rich in order to produce explosive deposits, but the volatile composition is at least partially lost upon eruption. The traditional view is that CO_2 is likely the dominant volatile species based on the depth of fluid exsolution and pressure-dependence of CO_2 solubility (Scott-Smith, 1996). A significant amount of carbonate in kimberlite groundmass is additional evidence for high CO_2 content. However, diamond dissolution experiments suggest that water is the dominant diamond solvent in kimberlite (Fedortchouk *et al*, 2007; Fedortchouk *et al*, 2008). This conclusion is supported by an observed excess of OH groups in kimberlitic olivine (Matveev and Stachel, 2007; Fedortchouk *et al*, 2008).

The Udachnaya-East kimberlite in Yakutia, Siberia has exceptionally unaltered portions (Kamenetsky *et al*, 2004; Kamenetsky *et al*, 2007). In the least altered parts of this kimberlite, highly soluble alkali chloride and carbonate minerals are abundant (*ca.* wt. 3%), occurring within the silicate groundmass and in carbonate-chloride nodules. These minerals show liquid immiscibility textures that can only be generated by crystallization from melts. The presence of melt inclusions of chloride-rich composition

(18.5 wt. %) in groundmass olivine supports a molten origin of these soluble alkali minerals (Kamenetsky *et al*, 2004; Kamenetsky *et al*, 2008). Maas *et al* (2005) measured strontium, neodymium and lead isotopes in Udachnaya-East silicates, alkali carbonates and chlorides, and infiltrating groundwater to test whether the alkaline minerals may have originated as secondary precipitates. The indistinguishable isotopic signatures of the silicate minerals and alkali carbonates and chlorides led to the conclusion that both mineral fractions originated from a common mantle source. Kamenetsky *et al* (2008) concluded, on the basis of Udachnaya-East olivine types and compositions and the unaltered mineralogy of this kimberlite, that parental kimberlite is an anhydrous chloride-carbonate melt that becomes contaminated by mantle olivine en route to the surface. The authors argue that evidence of extreme alkali and chloride enrichment is normally erased by dissolution during secondary deuteric fluid infiltration, which is also responsible for the H_2O-rich alteration minerals. This hypothesis is in contrast to the evidence supporting a free hydrous fluid phase as the primary diamond solvent in kimberlites (Fedortchouk *et al*, 2007; Matveev and Stachel, 2007; Fedortchouk *et al*, 2008). It would appear that the Udachnaya-East kimberlite is a mineralogically and compositionally unusual kimberlite.

Some diamonds have chloride-rich (10s of wt. %) brine inclusions (e.g., Izraeli *et al*, 2001; Tomlinson *et al*, 2006; Klein-BenDavid *et al*, 2007a). Although perhaps not directly applicable to kimberlites, these and other diamond fluid inclusions appear to define a ternary system between silicate-carbonate-chloride components with an immiscibility gap separating the silicate and chloride components (e.g., Safonov *et al*, 2007; Klein-BenDavid *et al*, 2007a). These data provide evidence for the co-existence of

chloride-rich fluids and diamonds in the diamond-forming environment in the mantle. Klein-BenDavid *et al* (2007a) suggested that fractionation in this ternary system could possibly give rise to the parental kimberlite melt. It is conceivable that these fluids may be related to Udachnaya-East kimberlite.

1.2 Diamonds

Diamonds are gemstones and important industrial materials derived principally from kimberlites. Diamonds are important geologically as physical records of mantle processes. Diamond is an isotropic mineral consisting of carbon atoms arranged in a face-centred cubic lattice. Each carbon atom is in tetrahedral coordination, bonded covalently to four other carbon atoms. The typical primary euhedral form of diamond is the octahedron, although cuboid diamonds are common and fibrous diamonds occur less commonly (Fedortchouk, personal communication). Octahedron faces are denoted in Miller notation as (111) (Figs. 1.2, 1.3). Octahedral diamonds change shape in response to dissolution, gradually evolving from the primary octahedral form to a final tetrahexahedoidal or hexoctahedroidal form as the (111) face is progressively dissolved (Fig. 1.2). The (111) face shape changes from a triangular to ditrigonal shape until complete dissolution. A hexoctahedron is a 48-sided polyhedron while a tetrahexahedron

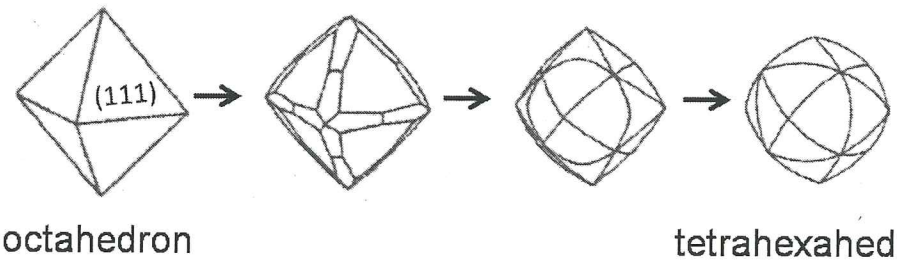

Figure 1.2: Morphological progression of a diamond octahedron with increasing dissolution. The (111) face gradually decreases in area as octahedron edges and vertices are dissolved to form a tetrahexahedroid (shown) or hexoctaherdoid. Note the change of in shape of the (111) face from triangular (left) to ditrigonal (left middle). After Khokhryakov and Pal'yanov (2007).

has 24 sides. The 'oid' suffix denotes that the faces of resorbed diamonds are not strictly planar crystallographic faces.

1.2.1 Diamond surface features

Natural diamond surfaces show a wide variety of geometric forms produced during growth and dissolution events. The most commonly occurring dissolution feature is the **negative trigon**, a triangular etch pit whose sides are rotated 60° from parallel to the edges of (111) faces (Fig. 1.3). **Positive trigons** (Fig. 1.3), whose sides are parallel to the edges of the (111) face, are much rarer. Both types of trigons can have flat or pointed bottoms (Fig. 1.3). **Hexagons** or hexagonal etch pits occur more commonly than positive trigons, but are less common than negative trigons. **Channels** are deeply penetrating etch pits of variable geometry. A variety of edge and vertex dissolution forms also occur. **Hillocks** are bumps occurring on resorbed edges that may have smooth or rough edges, and tend to have long dimensions running parallel to edges of (111) faces. **Disks** are

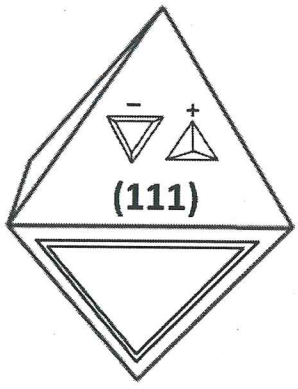

Figure 1.3: Octahedral diamonds typically display triangular etch pits (trigons) produced during dissolution events. Trigons can be negatively or positively oriented, and have flat or pointed bottoms. This sketch illustrates that the positive trigon ('+') has sides parallel to the edges of the (111) octahedron face, while the negative trigon ('-') is oppositely oriented. The negative trigon is shown as flat-bottomed, while the positive is point-bottomed. Trigons of any orientation can be pointed or flat-bottomed. The lower (111) face has a step face, a terrace-like feature that juts out of a lower (111) surface. These features are produced during both diamond growth and dissolution.

circular depressions in resorbed edges. **Corners** are angular protrusions having the same spatial orientation as octahedron vertices. **Striations** are parallel lines seen on smoothly resorbed edges and vertices. **Step faces** (Fig. 1.3) are terrace-like (111) faces that stick out of larger area faces – these can be growth or dissolution features. Graphitized diamond has been observed only once in nature (Tolansky, 1968).

Fedortchouk *et al* (2007) explored diamond dissolution in H_2O, CO_2 and H_2O-silicate melt systems at 1150-1500 °C and 1 GPa. They observed that dissolution in fluid-undersaturated melt results in surface graphitization of diamond, and therefore concluded that kimberlitic magma is accompanied by a free fluid phase, because graphitized diamond is exceedingly rare. Diamond dissolution features were shown to depend strongly on the composition of the solvent. H_2O-dissolved diamond has markedly different surface features than CO_2-dissolved diamond. Dissolution in H_2O produces rounded, striated edges with hillocks and disks. Few flat-bottomed negative trigons occur on (111) faces. Dissolution in CO_2 results in less edge dissolution, but pervasive trigon etching. Edge features are dominated by hillocks, while (111) faces are intensely etched by overlapping, somewhat irregular, negative flat-bottomed trigons. Importantly, dissolution in H_2O fluid in equilibrium with silicate melt results in less edge dissolution and a greater abundance of small negative trigons on the (111) faces than in pure H_2O fluid. The kinetics of dissolution were observed to be similar in all of these compositions.

Dissolution experiments presented by Kozai and Arima (2005) in kimberlitic, lamproitic and $MgCa(CO_3)_2$ solvents at 1300-1420 °C and 1 GPa produced contrasting surface features in different solvents. Interpreted in the context of their findings,

Fedortchouk *et al* (2007) argued that the contrasting surface features and dissolution kinetics reflect a differing fluid composition and low free fluid content, respectively. Diamond graphitization was observed in fluid-free $MgCa(CO_3)_2$ melts. Twenty minute runs in the H_2O- and CO_2-rich kimberlite solvents preserved octahedron geometry but produced a great number of tiny negative trigons on (111) faces.

Experiments by Khokhryakov and Pal'yanov (2008) at 1400-1750 °C and 5.7-7.5 GPa in CO_3^{2-}-H_2O, CO_3^{2-}-CO_2 and dry CO_3^{2-} systems confirmed that dissolution features depend on the composition of the solvent. In contrast to the results of Kozai and Arima (2005) at 1 GPa, dissolution in dry carbonate melt produced positive trigons, as opposed to surface graphitization. CO_2-oversaturated melt also produced positive trigons. Negative trigons were produced in H_2O-oversaturated melt, as were step faces and long hillocks. Some trigons appear to penetrate deep into the diamond, but detailed images of these features were not provided. Changes in diamond morphology were also dependent on the composition.

Dissolution experiments in NaCl and NaF melts at 1300-1350 °C and 3 GPa demonstrated that these solvents produce negative trigons on (111) faces, and graphitization upon carbon saturation in the melt (Sonin *et al*, 2008). However, absence of any correlation between reportedly very accurate diamond weight losses and experiment duration is difficult to explain if the solvent was actually the NaCl or NaF. It seems more likely that the solvent was one or more volatile components in air that were necessarily present as a contaminant, or by H-C species that can migrate freely through platinum capsules at the conditions of the experiments (Luth, 1993). Consumption of the free fluid at longer durations could then produce graphitization, as observed in fluid

undersaturated melts in other studies (Kozai and Arima, 2005; Fedortchouk *et al*, 2007).

1.2.2 Mechanism of diamond oxidation

Fedortchouk *et al* (2007) showed that diamond oxidation without graphitization requires the presence of a free fluid phase. They observed that activation energies of graphitization for different diamond faces corresponded to the energies of two and three carbon-carbon bonds, depending on the direction, while the activation energy of fluid-induced resorption is similar to the energy of one carbon-carbon bond. This observation is consistent with the oxidation model proposed by Rudenko *et al* (1979), where complexing between fluid molecules and open bonds on the diamond surface breaks carbon-carbon bonds in diamond one by one. The process of graphitization is then less energetically favourable, because two or three bonds must be broken at once. Thus when a free fluid phase is available to form complexes, dissolution will proceed without graphitization. In contrast, fluid molecules dissolved in silicate melt are not free to form complexes, and graphitization can occur. Fedortchouk *et al* (2007) also speculated that the face-dominated etching produced in CO_2 fluid, as compared to the edge-dominated dissolution in H_2O, may result from contrasting molecular geometries and differing open bond distances in different directions in the diamond lattice.

Dissolution sites, such as trigons and channels, are often postulated to occur where crystal defects, such as dislocations, outcrop on the diamond surface (Lu *et al*, 2001; Klein-BenDavid *et al*, 2007b). This hypothesis has not been tested experimentally. However, the greater incidence of trigons produced by free fluid in equilibrium with melt (Fedortchouk *et al*, 2007) compared to hydrous fluid alone indicates that the compositional environment plays at least some part in determining the number of etch

sites on the (111) face.

1.3 Investigating chloride in kimberlites using diamond surface features

The proposed anhydrous chloride-carbonate-silicate primary kimberlite composition of Kamenetsky *et al* (2008) is very different from the ideas of numerous other authors (e.g., Matveev and Stachel, 2007; Fedortchouk *et al*, 2007; Fedortchouk *et al*, 2008; Mitchell, 2008; Francis and Patterson, 2009). Although the work of Sonin *et al* (2008) did explore the effect of sodium salts on diamond dissolution features, mounting evidence of high water content in kimberlites warrants investigation at intermediate compositions between chloride and water end members. The purpose of this investigation was to determine whether NaCl-H_2O and KCl-H_2O fluids produce distinctive dissolution features on diamonds at 1350 °C and 1 GPa. These conditions were chosen to match those of Kozai and Arima (2005) and Fedortchouk *et al* (2007). Given that fluid composition strongly influences dissolution features, it is expected that surface features will depend on the fluid composition in these two systems. However, since diamond dissolves by oxidation, and neither NaCl nor KCl are likely oxidizing agents, little effect is expected in the end member salt compositions. At intermediate compositions, a dilution-effect is expected resulting from reduction of water activity. If chloride-water fluids can generate distinctive surface forms on diamond, then natural diamond surfaces can be investigated to evaluate the significance of chloride-rich fluid in kimberlite systems. As part of a growing dataset covering diamond dissolution features and processes, this work also aims to help elucidate the mechanism of diamond oxidation. The results may be more broadly applicable to evaluate the effect of solutes on fluid-induced dissolution. Finally, dissolution features may be relevant to the fluid

composition of the subcontinental mantle itself given the evidence for chloride-rich mantle brines from fluid inclusions in diamonds. Although these fluids are typically discussed in the context of diamond growth, the suggestion of Klein-BenDavid *et al* (2007a) that kimberlite origins may be related to mantle brines makes investigations of chloride-diamond interactions especially interesting.

CHAPTER 2: MATERIALS AND METHODS

2.1 Overview

Diamond dissolution was studied in the systems H_2O-NaCl and H_2O-KCl at 885 °C and 101 kPa[1], and at 1350 °C and 1 GPa[2] to examine the effect of Cl^--H_2O fluids on diamond dissolution features. The conditions of 1 GPa experiments are similar to those of Arima *et al* (2005) and Fedortchouk *et* al (2007). At 101 kPa, the effect of molten NaCl on diamond dissolution was investigated, while a wider array of compositions was explored at 1 GPa (Fig. 2.1).

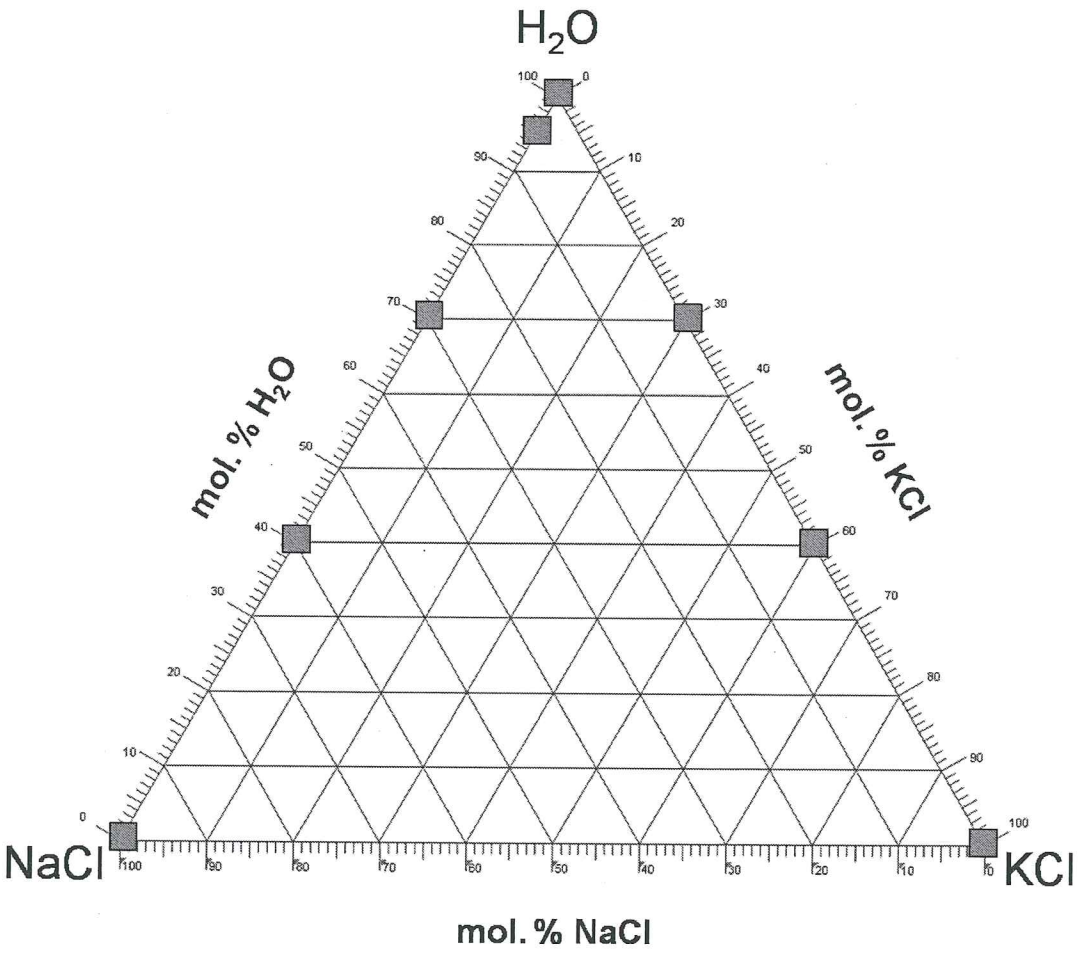

Figure 2.1: Ternary plot of molar fluid compositions studied in 1 GPa experiments. Only NaCl was investigated at 101 kPa. The error in starting compositions was smaller than the area of the symbols.

[1] 101kPa is atmospheric pressure.
[2] 1 GPa is equivalent to lithostatic pressure at about 30 km depth.

2.2 Sample selection and preparation

Diamonds were selected from a micro-diamond (< 1 mm) exploration parcel from the Misery Kimberlite, Lac de Gras Kimberlite Field, Northwest Territories, Canada[3]. Hexoctahedroidal diamonds were selected for 101 kPa experiments, while flat-faced unresorbed octahedral diamonds with few dissolution features were chosen for high pressure experiments. In general, diamonds with strong colour, inclusions or cracks were avoided. However, the octahedral diamond population was small and ideal diamonds were uncommon, so some flexibility was permitted during sample selection. Each side of all diamonds was photographed with an optical microscope under reflected light. Diamonds were cleaned ultrasonically in methanol or ethanol and weighed prior to use.

Although the scale used is very accurate (*ca.* ± 0.02 mg), some spurious weight measurements were encountered. These may be attributed to vibrations, small changes in air pressure and user error.

2.3 Reagents and starting compositions

Starting compositions for the experiments were composed of mixtures of $Mg(OH)_2$ (95-100.5% purity, Alfa Aesar) and NaCl (>99.0% purity, ACP) or KCl (>99.995% purity, Alfa Aesar), . $Mg(OH)_2$ was selected as the water source because it breaks down to MgO_{solid} and H_2O_{fluid} below 1000 °C. All reagents were of a minimum of 99% purity.

Reagents for 1 GPa experiments were ground to a powder with a mortar and pestle for 10-20 minutes to enhance packing into capsules. Two component mixtures were ground in an ethanol suspension to enhance homogeneity of the mixture. NaCl used in atmospheric pressure experiments was not ground. All reagents were dried in an oven

[3] Micro-diamond parcel provided by BHP Billiton Diamonds, Incorporated.

at 100 °C overnight or longer to drive off excess ethanol and water.

2.4 101 kPa experiments

101 kPa experiments were conducted in a Vulcan 3-550 furnace, which can attain temperatures up to 1100 °C. The furnace was calibrated against NaCl, K_2CO_3 and Na_2CO_3 melting points. Reagents were placed in a crucible and heated to a run temperature above the melting point. The sample was observed after cooling. If the sample converted to a glass filling the base of the crucible, the sample melted during the run. If it remained crystalline and porous, no melting occurred. These experiments demonstrated that the temperature achieved at run conditions was about 10-20 °C lower than that indicated on the display screen (data not shown). Here, temperatures are given with a -15 °C correction.

In diamond dissolution experiments (Fig. 2.2), NaCl was placed in an Al_2O_3 crucible. The mass of NaCl depended on the size of the crucible used – *ca.* 1 g in small crucibles and *ca.* 10 g in medium crucibles – so that the reagent was sufficiently deep to completely cover the small diamond. The diamond was inserted into the NaCl using tweezers. The small or medium crucible was placed inside a large crucible and both were covered with Al_2O_3 lids. The same type of setup was used to test the effect of air.

In each run, the furnace was preheated to 585 °C. The crucible assembly was placed in the furnace near the centre. The temperature was raised to 885 °C for 15-1300 minutes. Run durations were 60-1300 minutes in NaCl and 15 minutes in air. The furnace was cooled to 585 °C prior to specimen removal. After allowing time for the crucibles to cool, the solidified NaCl was dissolved away using warm water. The recovered diamond was cleaned ultrasonically in methanol or ethanol and water, weighed

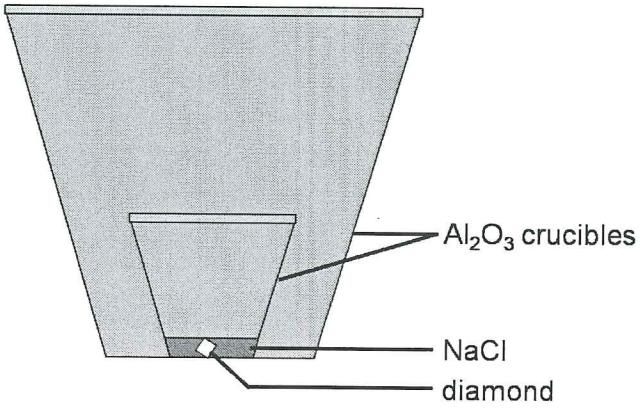

Figure 2.2: Experimental setup for 101 kPa experiments. Diamond was placed in NaCl inside two closed alumina crucibles. For the air experiment, diamond was not placed in any reagent.

and photographed.

2.5 1 GPa experiments

This piston-cylinder (PC) apparatus was used for experiments at 1 GPa and 1350 °C. The PC generates high pressures by pumping oil against a large diameter piston via an electric motor. Force applied to this piston is transferred to a small diameter piston. The transmission of force from a larger area to a much smaller one generates high pressures (up to ca. 3.5 GPa) suitable for geological studies. High temperatures are obtained by passing an electric current through a graphite heater that surrounds the sample.

2.5.1 Apparatus' structure and function

Physical PC components of particular interest are contained within the pressure plate, which is depicted in Figure 2.3a. The most important components are the small tungsten carbide (WC) piston, which pressurizes the cell assembly, and the hardened steel and WC bomb. The bomb encloses the sample and remains rigid at run conditions so that

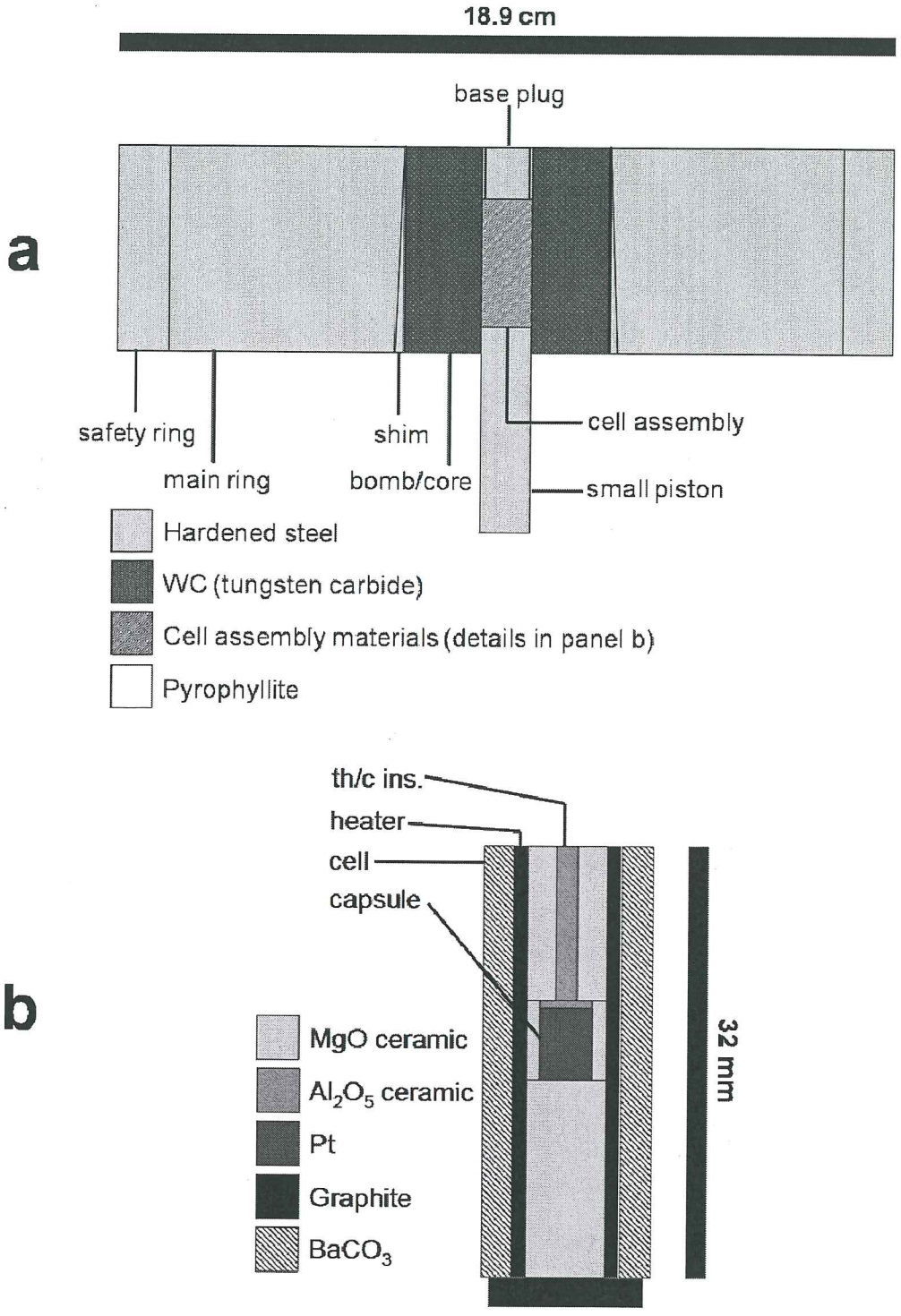

Figure 2.3: Pressure plate of the piston-cylinder (a) and cell assembly (b) used in 1 GPa experiments. Components and their materials are labeled. th/c ins.: thermocouple insulator. Components are shown to scale. After Dunn (1993).

the pressure exerted on the cell assembly is not alleviated by deformation of the surrounding medium. The cell is composed of a weak material (*e.g.*, $BaCO_3$, NaCl, talc) that transmits nearly lithostatic pressure to the sample at high temperature and stress. The graphite furnace and sample are contained within the cell, into which a thermocouple is inserted to measure the temperature. Thermocouples consist of two wires of different composition that heat at differing rates when pressed against a heat source. A temperature-dependent voltage difference, or electromotive force, is generated between the wires. The electromotive force is measured and converted to temperature by a controller (Dunn, 1993).

All PCs expose cell assemblies to a temperature gradient, *i.e.* the temperature is highest where the graphite heater connects to the electric current and decreases away from that location. The area of highest temperature is known as a hot zone, and its position must be calibrated for every PC. The position of the hot zone was determined from the thickness of a spinel layer that forms between the Al_2O_3 thermocouple insulator and the MgO ceramic enclosing the capsule (Fig. 2.3b) (Watson et al., 2002).

The cell assembly for these experiments consisted of a $BaCO_3$ cell, a graphite heater, MgO ceramic space-filling pieces and a basal graphite disk (Fig. 2.3b). The sample was contained in a platinum capsule. A W-Re thermocouple protected by an Al_2O_3 insulator was used to measure the temperature. The thermocouple tip is decoupled from the capsule with a small Al_2O_3 disk.

2.5.2 Pressure correction

In PC experiments certain cell types require pressure corrections. These corrections are necessary because friction between the cell assembly and the bomb resists

the pressure applied by the small piston, and because cell materials do not transmit perfectly lithostatic pressure to the sample due to finite material strength. Such pressure corrections are usually termed a *friction correction* (Dunn, 1993). In the case of $BaCO_3$, application of a 5% friction correction to the applied pressure typically exerts the desired pressure on the sample (McDade et al., 2002). The desired pressure in these experiments is 1 GPa, so we apply a pressure of 1.05 GPa. It should be noted that the friction correction should be determined for the specific PC as well as the cell type. This work is ongoing at Dalhousie's Experimental Petrology Lab using the melting point of NaCl (Bohlen, 1984), so for the time being a correction of 5% is a reasonable approximation.

2.5.3 Sample preparation and setup

Platinum capsules were loaded with ground reagent and the diamond. Reagent was packed tightly in the capsule using a brass or steel rod. Capsules containing mixtures of ≥30 mole % alkali chlorides were stored at ≥ 100 °C overnight or longer to ensure evaporation of absorbed water. Capsules were sealed by arc-welding to preserve fluids produced during the experiment. Capsules and other cell assembly parts were then assembled according to the order shown in Fig 2.2b. The cell assembly and other PC pieces were assembled according to Fig 2.2a.

2.5.4 Procedure

The run conditions (1350 °C, 1 GPa) were achieved in a few steps. Pressures given here represent the friction-corrected pressure acting on the small piston, not the hydraulic pressure applied to the large piston. Pressure was initially increased to *ca.* 200-350 MPa at room temperature. Temperature was increased at *ca.* 100 °C / min to 600 °C,

where it would remain for 6 min. During that interval, pressure was increased to ca. 1.05 GPa. Temperature was increased at 100 °C /min to the final temperature of 1350 °C. Pressure was adjusted back to 1.05 GPa at 900 and 1350 °C.No additional pressure adjustments were made for the duration of the run (60 minutes), with the exception of run PC-48, for which a readjustment to 1.05 GPa was applied when pressure dropped below 0.8 GPa during the run. The system was quenched at the end of the run by shutting off the power. Temperature decreased to room temperature within tens of seconds of quenching. Pressure generally decreased during experiments to ca. 0.8-0.9 GPa.

Diamonds were recovered from the cell assembly and capsule using vice grips, wire cutters and tweezers. Diamonds were cleaned ultrasonically in ethanol and sometimes water for at least five minutes. The diamond was weighed and photographed.

2.6 Scanning electron microscopy

Diamonds from low and high pressure experiments were imaged using a Hitachi S-4700 FEG Scanning Electron Microscope at the Institute for Research in Materials, Dalhousie University. Samples were cleaned ultrasonically in ethanol for at least 5 minutes, and then mounted on a metal stub using carbon-based adhesive. Sample stubs were carbon-coated at the Dalhousie Regional Microprobe Facility. Samples were imaged under a 12 μA operating current and 5-7 kV accelerating voltage at a working distance of 12 mm. Note that these values tended to shift slightly during operation. Graphitized diamonds from 1 GPa NaCl runs were imaged both before and after removal of the graphite. Graphite was removed by heating the diamonds to 500 °C for two days.

CHAPTER 3: RESULTS

3.1 Diamond dissolution experiments in NaCl and air at 101 kPa, 885 °C

Diamond dissolution was studied in molten NaCl and air at 885 °C and 101 kPa (Table 3.1). The 60, 180 and 1300 minute experiments produced similar dissolution forms (Fig. 3.1), while no significant weight loss was observed (Table 3.1). Micron-scale bumps were the dominant features formed under these conditions. These bumps appear to share a common direction of elongation. Diamond exposed to air for 15 minutes at the same conditions showed similar features (Fig. 3.1), although much greater weight loss occurred under these conditions. These bumps are larger than those produced in NaCl experiments. Channels were observed on the NaCl-treated diamonds when viewed with a scanning electron microscope. However, it is unclear whether these features were produced during the experiment.

3.2 Diamond dissolution experiments in H_2O-Cl^- Systems at 1 GPa, 1350 °C

Diamond dissolution was studied in NaCl- H_2O and KCl -H_2O fluids at 1 GPa and 1350 °C (Table 3.2). In general, diamond dissolution was characterized by rougher features in chloride-bearing fluids than in pure water. KCl-bearing aqueous fluids produced smoother features than NaCl-bearing fluids. NaCl-bearing fluids produced a greater number of trigons on (111) faces than equivalent KCl-H_2O fluids.

3.2.1 Diamond surface features produced in H_2O fluid

Dissolution features produced by H_2O fluid in this study were consistent with those reported by Fedortchouk *et al* (2007) (Fig. 3.2). Insignificant weight loss was accompanied by rounding of vertices and edges forming dominantly smooth edges.

Run	Sample	Composition (mole %)	Temperature (°C)	Pressure	Time (min)	Start weight (g)	End weight (g)	Weight loss (g)	Weight loss (%)	Surface etching	Surface graphitization
V-02	S08-02	100% NaCl	885	101 kPa	60	1.95	1.99	-0.04	-2.05	X	
V-25	S08-25	100% NaCl	885	101 kPa	180	2.16	2.12	0.04	1.85	X	
V-26	S08-26	100% NaCl	885	101 kPa	1300	1.33	1.32	0.01	0.75	X	
V-07	S08-13	air*	885	101 kPa	15	0.88	0.63	0.25	28.41	X	
PC-17	D08-02	100% H_2O	1350	1 GPa	60	1.68	1.54	0.14	8.33	X	
PC-36	D08-08	95% H_2O, 5% NaCl	1350	1 GPa	60	0.66	0.66	0	0.00	X	
PC-22	D08-05	70% H_2O, 30% NaCl	1350	1 GPa	60	1.32	1.33	-0.01	-0.76	X	X
PC-26	D08-06	40% H_2O, 60% NaCl	1350	1 GPa	60	1.92	1.92	0	0.00	X	X
PC-20	D08-03	100% NaCl	1350	1 GPa	60	2.10	2.07	0.03	1.43	X	X
PC-41	D08-10	100% NaCl	1350	1 GPa	60	1.81	1.74	0.07	3.87	X	X
PC-34	D08-09	70% H_2O, 30% KCl	1350	1 GPa	60	0.65	0.62	0.03	4.62	X	
PC-48	D08-15	40% H_2O, 60% KCl	1350	1 GPa	60	0.74	0.73	0.01	1.35	X	X
PC-27	D08-07	100% KCl	1350	1 GPa	56	0.62	0.67	-0.05	-8.06	X	X

Table 3.1: Summary of conditions for all experiments. All samples were partially dissolved during experiment. See Section 2.2 for a discussion of the accuracy of the weight and weight loss measurements. * Dry air is 78% N_2, 21% O_2 and 1% other gases, including Ar and CO_2. Some water vapour would also be present in the air. X indicates the presence of the relevant feature.

Run	Sample	Composition (mole %)	Trigons	Hexagons	Step faces	Striations	Hillocks	Disks	Corners	Graphitization
PC-17	D08-02	100% H_2O	large negative FB, PB		X	X	X	X		
PC-36	D08-08	95% H_2O, 5% NaCl	large negative FB		X	X	X	X	X	
PC-22	D08-05	70% H_2O, 30% NaCl	medium negative FB		X		X	X	X	X
PC-26	D08-06	40% H_2O, 60% NaCl	small negative FB	X			X	X	X	X
PC-20 PC-41	D08-03 D08-10	100 % NaCl	small positive PB, FB	X						X
PC-34	D08-09	70% H_2O, 30% KCl	FB - large	X	X		X		X	
PC-48	D08-15	40% H_2O, 60% KCl	medium negative FB	X	X		X		X	X
PC-27	D08-07	100% KCl	small positive PB	X						X

Table 3.2: Summary of dissolution features produced on diamond during 1 GPa experiments. X indicates the presence of a feature. FB: flat-bottomed. PB: Point-bottomed.

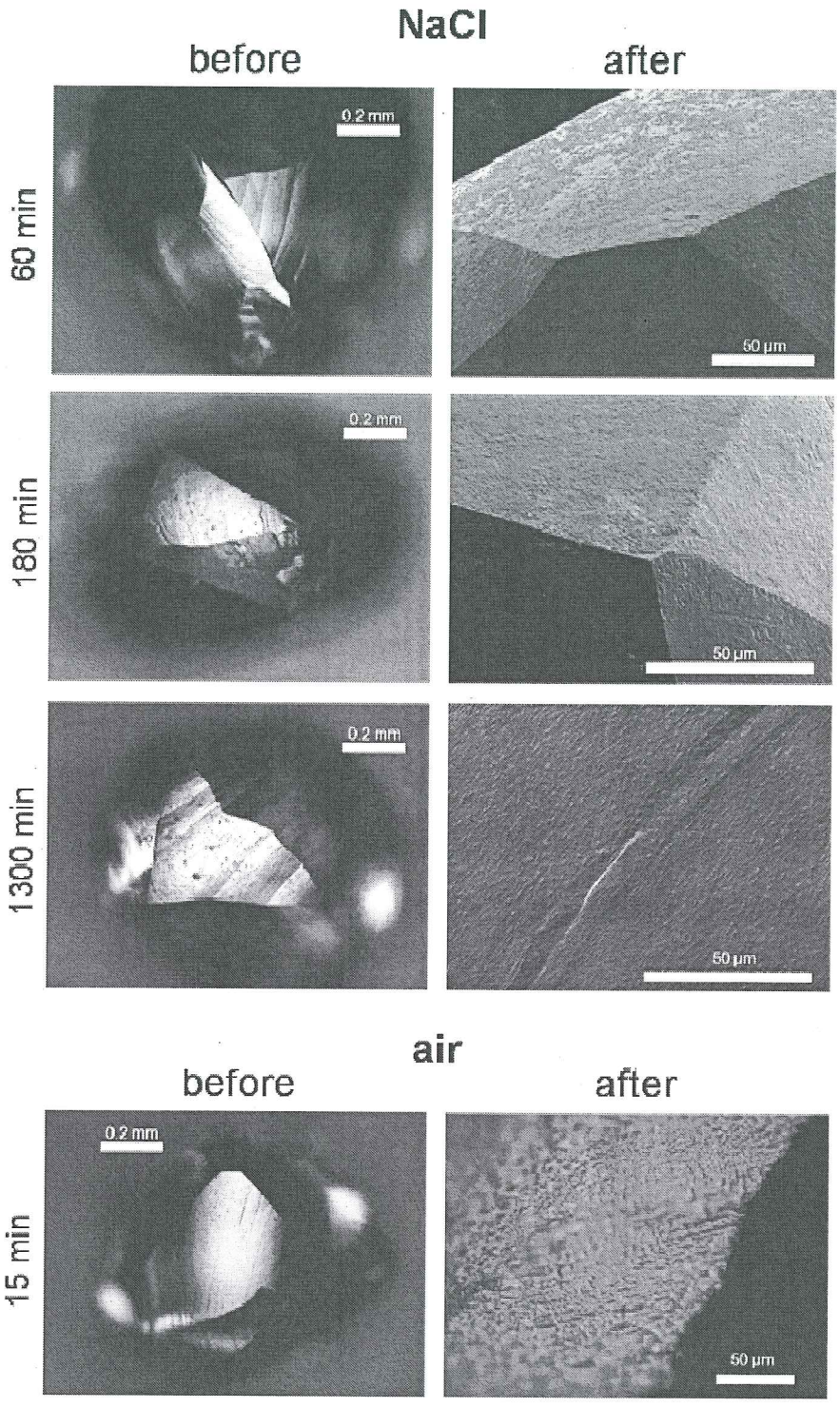

Figure 3.1: Diamond surface features produced in molten NaCl and air at 885 °C and 101 kPa. The amount and appearance of micron-scale bumps is similar at 60, 180 and 1300 minute exposure times in NaCl melt. Similar features were produced by oxidation in air for 15 minutes. Starting diamonds and the air-oxidized sample were photographed under reflected light. Results were imaged using a scanning electron microscope, except for the air-exposed diamond, which was photographed under reflected light. The 'after' images are at higher magnification (see scale bars).

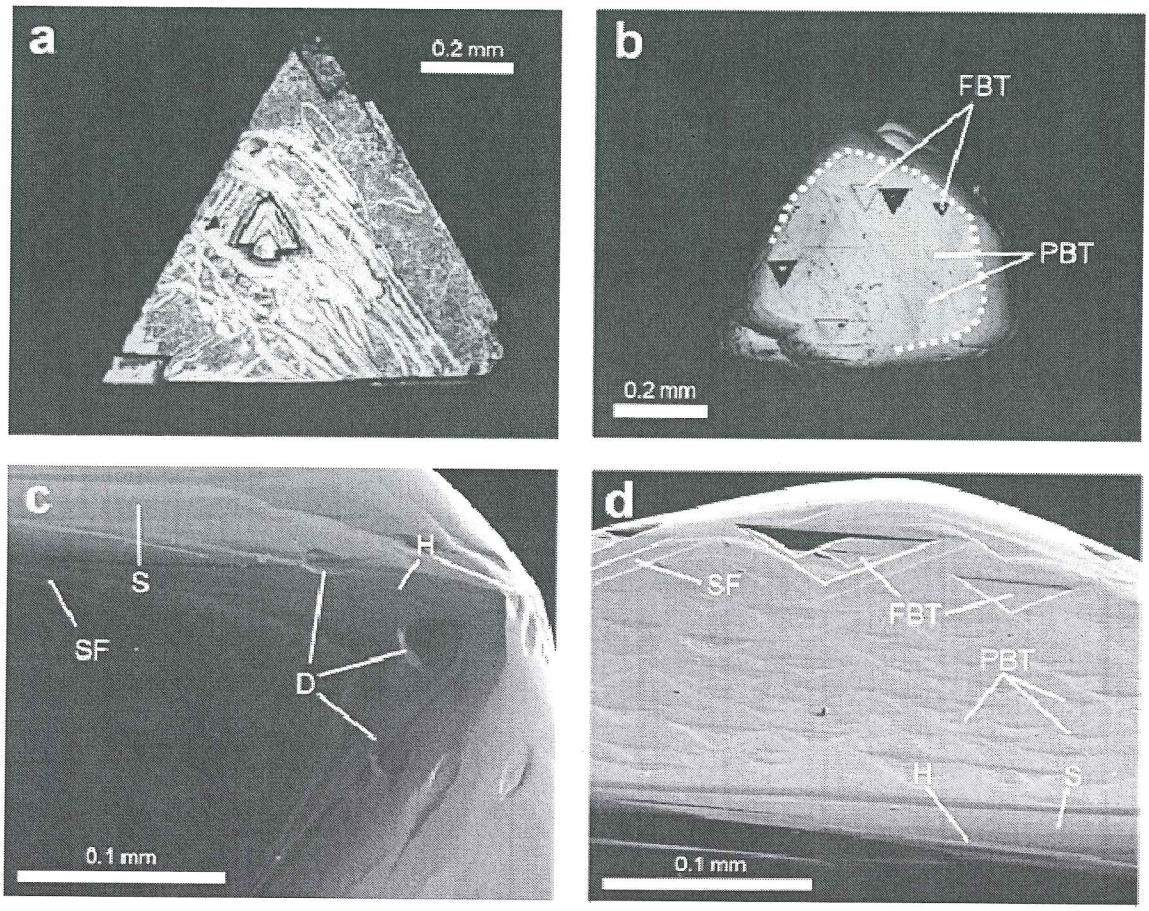

Figure 3.2: Representative images of diamond surface before (a) and after (b, c, d) exposure to H_2O fluid for 60 minutes at 1350 °C and 1 GPa. H_2O fluid produces smoothly rounded edges and vertices. Faces show large flat-bottomed trigons and smaller point-bottomed trigons. Step faces are also observed. Edge features include striations, hillocks and disks. Faces show a ditrigonal shape. Images are reflected light photographs (a, b) and scanning electron micrographs (c, d) summarizing the results from one experiment (run PC-17). D: disk. FBT: flat-bottomed trigon. H: hillock. PBT: point-bottomed trigon. S: striation. SF: step face. Dashed line: ditrigonal face.

Additional edge features included striations, hillocks and disks. (111) faces were characterized by few large, negative flat-bottomed trigons and many smaller point-bottomed trigons. The geometry of the face itself transformed from the triangular octahedron face to a ditrigonal form. Step faces were also observed.

3.2.2 Diamond surface features produced in NaCl-H_2O fluids

Addition of NaCl to aqueous fluid significantly affected the surface features generated on diamond (Fig. 3.3). Edge dissolution was both pronounced and smooth in H_2O-rich

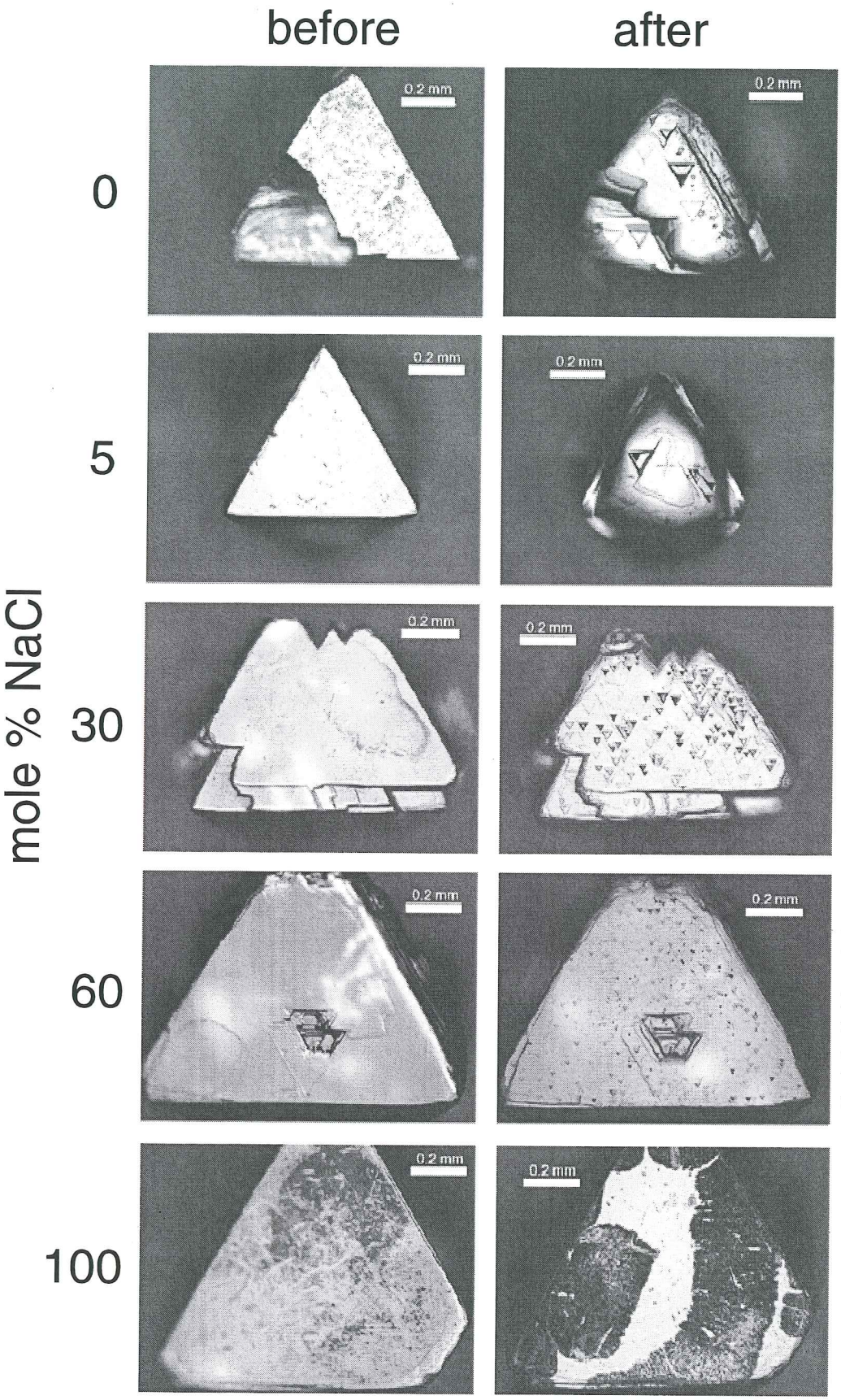

Figure 3.3: General view of diamond surfaces before and after exposure to NaCl-H_2O fluids for 60 minutes at 1350 °C and 1 GPa. Less surface etching occurs as the NaCl fraction increases. Focus of dissolution changes from edges to faces with the addition of NaCl. The number of trigons increases with the addition of NaCl and their size decreases. In 100% NaCl, about half of the diamond surface graphitized. Numbers denote molar percentages of NaCl. Images taken under reflected light.

compositions. Addition of 30 and 60% NaCl tended to produce a greater number of trigons on octahedron faces and rougher edge features, and largely preserved the (111) face geometry. Small amounts of graphitization were observed on diamonds exposed to intermediate compositions, while about half of the surface was graphitized by molten NaCl.

5% NaCl fluid

Dissolution features produced by 5% NaCl fluid were similar to those produced by water (Fig. 3.4). Edges and vertices were strongly smoothed and featured striations, hillocks and disks. One patch of angular corners was observed. (111) faces featured few, large, negative flat-bottomed trigons. Octahedron faces tended to transform from triangular to ditrigonal shapes. Step faces were also generated in this fluid composition. These features are indistinguishable from those reported by Fedortchouk *et al* (2007) for water.

30% NaCl fluid

Dissolution in 30% NaCl resulted in insignificant weight loss. Resorption features produced by 30% NaCl fluid differed significantly from those produced by H_2O-rich compositions discussed above (Fig. 3.5). Edge dissolution was severely reduced and the edge features were rougher in appearance. Hillocks were the dominant edge feature, while corners were common at vertices. A few disks were also observed near vertices. A new structure, tentatively called *crater-and-mound*, formed near two vertices. This structure consisted of a crater-like depression with ridged walls and a mound of graphite at the crater's centre. Ridges were not strictly linear features but shared a similar orientation.

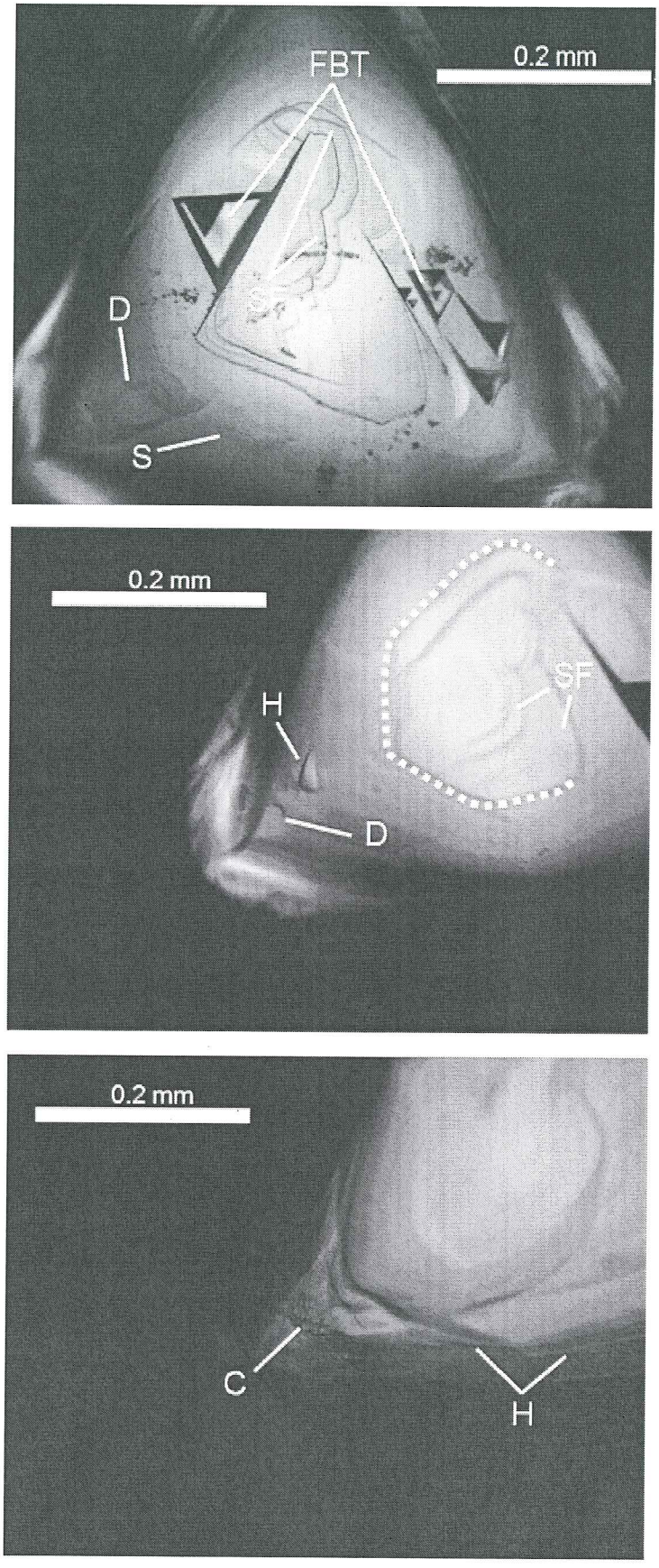

Figure 3.4: Diamond surface after exposure to 5% NaCl aqueous fluid for 60 minutes at 1350 °C and 1 GPa. Edges and vertices are smoothly rounded and few, large, flat-bottomed negative trigons developed on faces. Some step faces are present. Other edge and vertex features include disks, striations, hillocks and one patch of sharp corners. Faces show ditrigonal shape. Diamond was photographed under reflected light. Images shown represent surface features produced in one experiment (run PC-36). C: corners. D: disks. FBT: flat-bottomed trigons. H: hillocks. S: striations. SF: step faces. Dashed line: ditrigonal face.

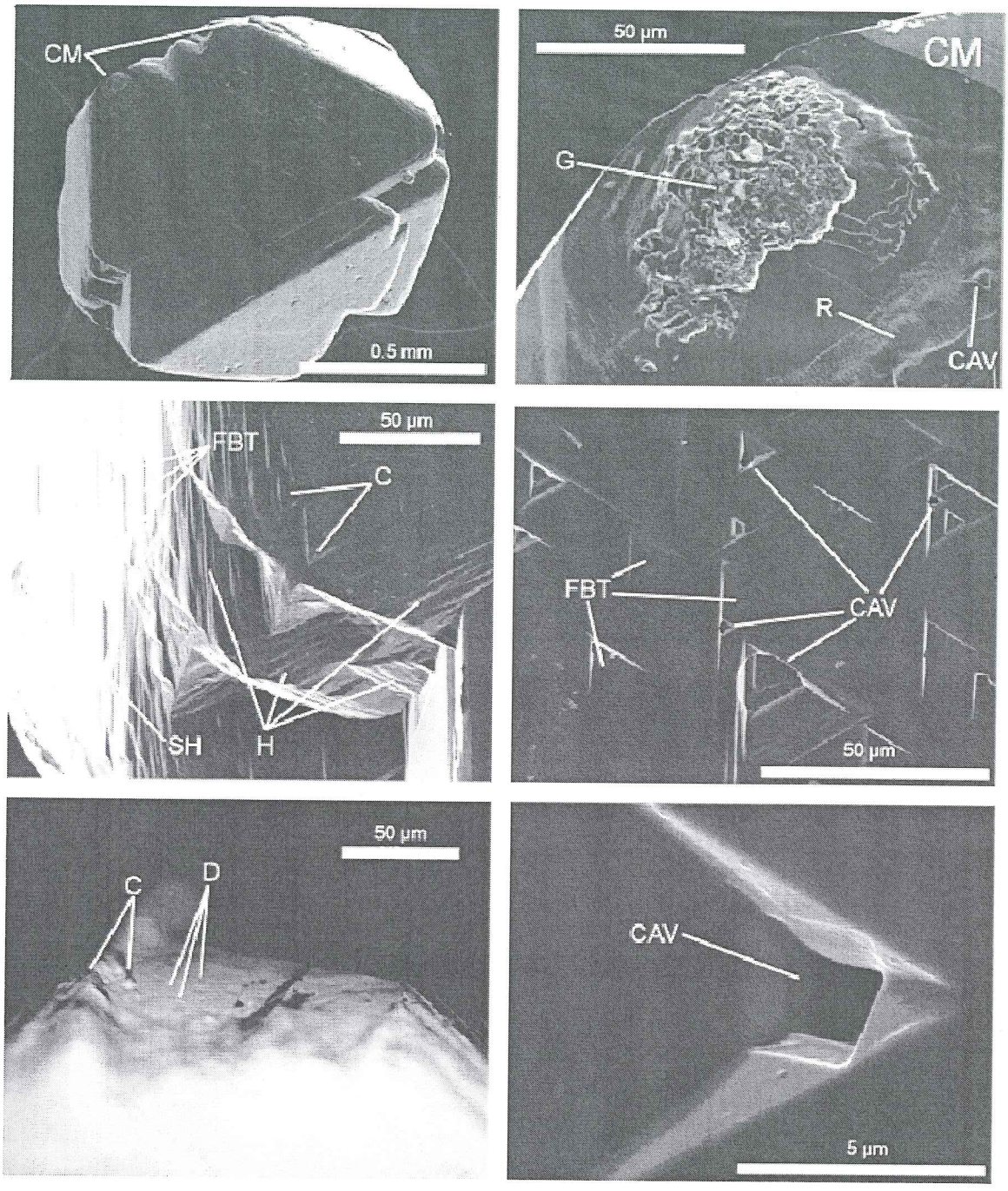

Figure 3.5: Diamond surface after dissolution in 30% NaCl aqueous fluid for 60 minutes at 1350 °C and 1 GPa. (111) faces are dominated by many small, negative, flat-bottomed trigons with fewer complex cavities. Cavities are confined within trigons. Hillocks dominate the edges. Vertices feature sharp corners, disks and crater-and-mound structures. Crater-and-mound structures (upper right) consist of ridge-like features on the walls of crater-like depressions with mounds of graphite at their centres. Diamond imaged by reflected light photography (lower right) and scanning electron microscopy (all others). Images represent surface features produced in one experiment (run PC-22). C: corners. CAV: cavities. CM: crater-and-mound. D: disks. FBT: flat-bottomed trigon. G: graphite. H: hillock. R: ridges.

The density of flat-bottomed trigons increased on (111) faces, while the size of trigons decreased compared to H_2O-rich conditions (Figs. 3.5 and 3.4). Small, deep, geometrically complex cavities resembling channels were found within some trigons. These cavities ranged from hexagonal to more complex polygonal cross-sections. Irregular deviations from polygonal cross-sections were also observed.

60% NaCl fluid

Exposure to 60% NaCl fluid produced insignificant weight loss. Dissolution produced very few edge features leading to overall preservation of the (111) face (Fig. 3.6). Most edge dissolution features were concentrated near vertices and included a few corners, normally shaped hillocks as well shapeless hillocks. Shapeless hillocks had irregular forms and deviated from a common elongation direction.

60% NaCl fluid produced abundant flat-bottomed trigons (Fig. 3.6) smaller than those produced by 30% NaCl fluid (Fig. 3.5). Some trigons exhibited hexagonal truncations. Small complex cavities similar to those produced in 30% NaCl appeared within some trigons. One face showed small spots of graphite.

NaCl melt

Dissolution in molten NaCl resulted in insignificant weight loss. Surface features produced in molten NaCl at 1GPa and 1350 °C contrast to those described above from 101 kPa experiments (Figs. 3.7 and 3.1). A few shapeless hillocks were produced on edges and vertices. About half of the diamond surface was graphitized. Graphite morphology was heterogeneous, ranging from sub-hexagonal tabular crystals to porous sheets. Removal of graphite showed that graphitization was associated with irregular,

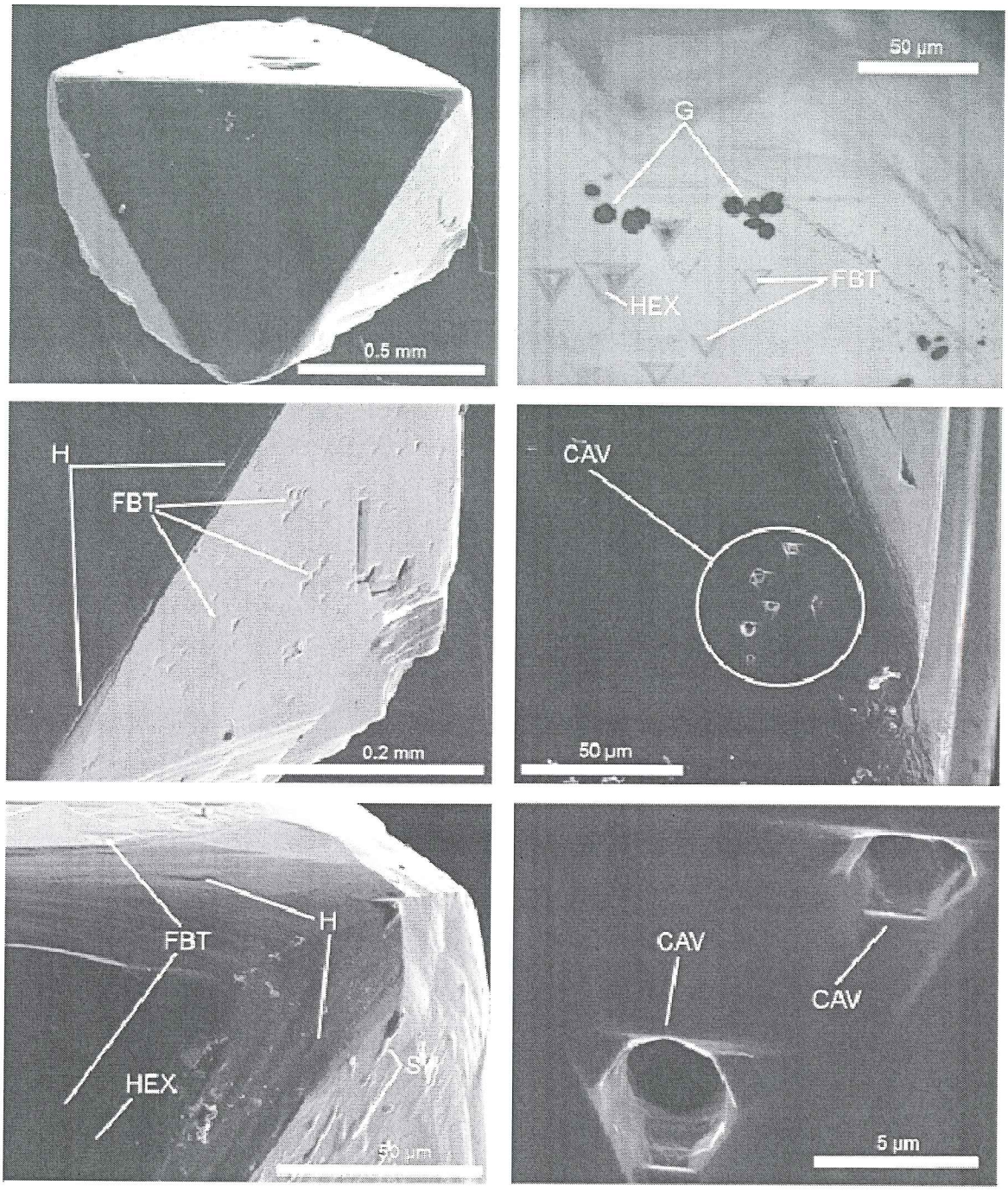

Figure 3.6: Diamond surface after dissolution in 60% NaCl aqueous fluid for 60 minutes at 1350 °C and 1 GPa. The octahedron shape remains largely preserved. Abundant small, negative, flat-bottomed trigons appear on (111) faces. Some trigons exhibit hexagonal truncations. Complex, deep cavities are associated with some trigons. Both ordinary and shapeless hillocks occur on dissolved edges. Small growths of graphite are present on one face. Diamond was imaged using reflected light photography (upper right) and scanning electron microscopy (all others). Images shown represent surface features produced in one experiment (run PC-26). CAV: cavities. FBT: flat-bottomed trigons. G: graphite. H: hillocks. HEX: trigons with hexagonal truncation. SH: shapeless hillocks.

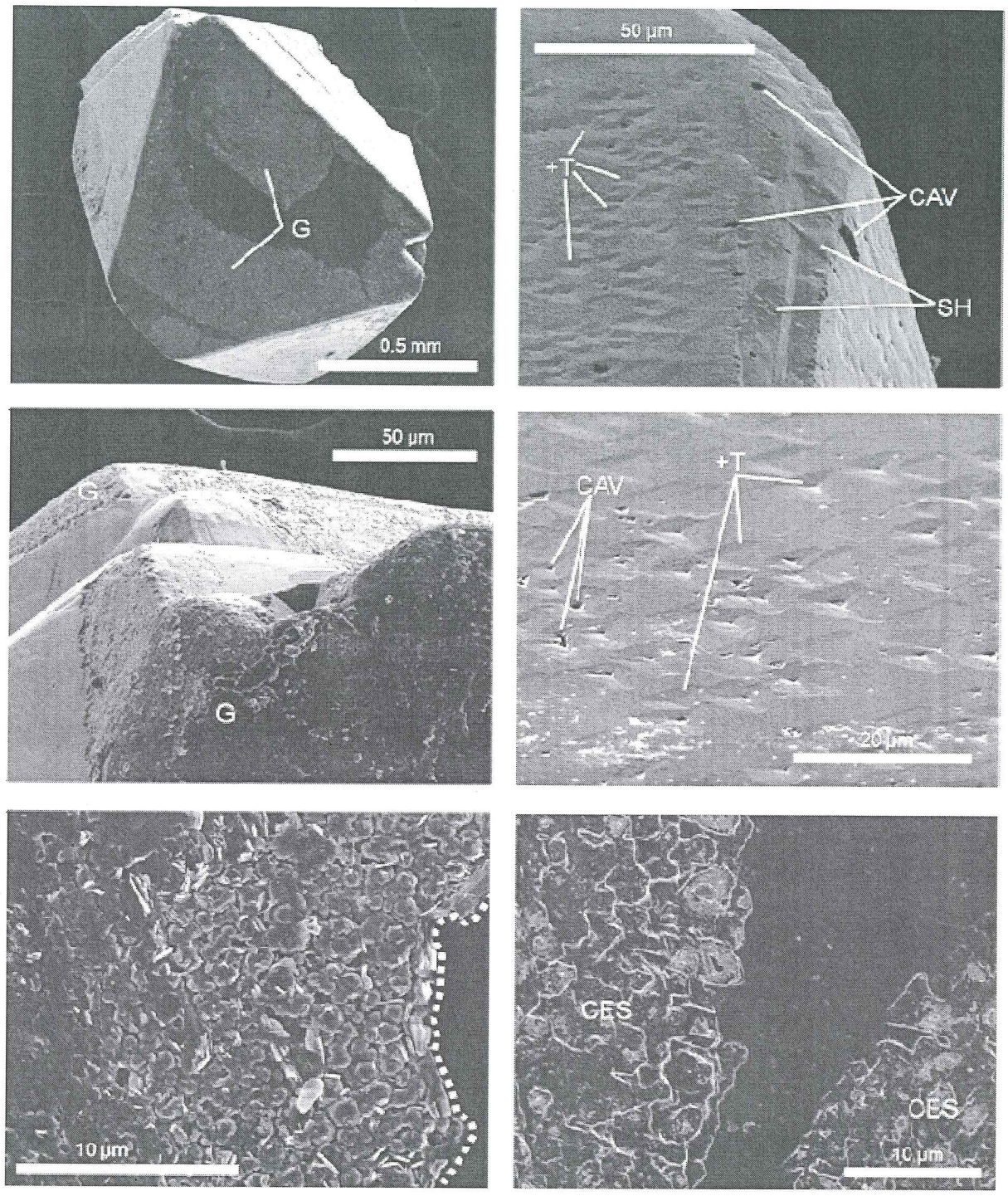

Figure 3.7: Diamond surfaces after dissolution in NaCl melt for 60 minutes at 1350 °C and 1 GPa. Graphite covers about half the surface in rounded areas. Graphite morphology is heterogeneous and complex. Graphite removal reveals complex etch surfaces underlying graphitized areas (lower right). Etching away from graphitized surfaces is dominated by positive trigons and cavities. Diamonds were imaged by scanning electron microscopy. Images shown represent surface features produced in two experiments (runs PC-20, PC-41). In the lower left panel, everything left of the dashed line is graphitized surface. +T: positive trigons. CAV: cavities. CES: complex etch surfaces. G: graphite.

complex etching. Graphite tended to be concentrated in rounded areas and showed no special affinity for vertices, edges or faces. Other areas on octahedral faces featured abundant, small, positive point-bottomed and flat-bottomed trigons. The occurrence of positive trigons was not observed in other NaCl-bearing compositions, and is uncommon on natural diamonds. Irregular, deep cavities were observed on edges and (111) faces. The overall octahedral shape remained well-preserved.

Summary

In general, NaCl-bearing aqueous fluid dissolved diamond differently than water. Although no effect is observed at 5% NaCl, the presence of 30-60% NaCl strongly reduced the amount of edge dissolution, and produced a high density of small trigons on (111) faces. Channel-like cavities were produced in these compositions. Diamond developed large patches of graphite associated with irregular dissolution surface in NaCl melt. The formation of positive trigons away from graphitized areas in this condition is unusual for natural diamonds.

3.2.3 Diamond surface features produced in KCl-H_2O fluids

KCl-bearing fluids produced contrasting features to both water and NaCl-H_2O fluids (Figs. 3.8, 3.2, 3.3). 30-60% KCl fluids produced rougher edge features than water. 60% KCl produced a higher density of trigons on (111) faces than H_2O. In general, KCl-bearing fluids produced smoother features with fewer trigons than equivalent NaCl-aqueous fluids. Molten KCl produced a few rounded areas with complex etch cavities and graphite, with shallow hexagons and positive trigons, and cavities on (111) faces away from the graphitized areas.

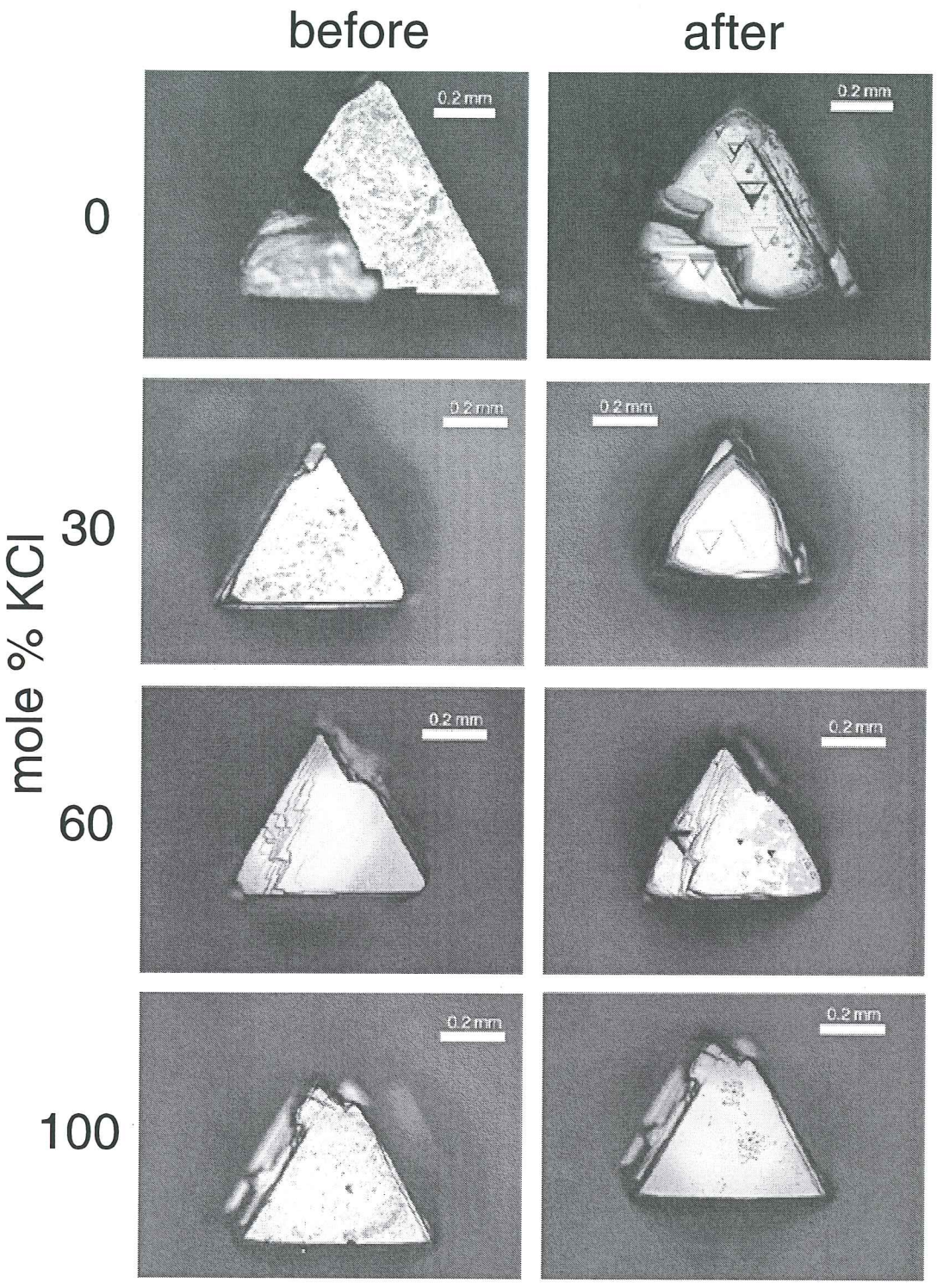

Figure 3.8: General view of diamond surfaces before and after exposure to KCl-H_2O fluids. Less surface etching occurred as the KCl fraction was increased. Surface etching was concentrated on edges and vertices in H_2O-rich conditions. Character of edge features was rougher at intermediate compositions. Etch cavities produced in molten KCl were concentrated in rounded areas on faces and edges, and included etch pits and graphite deposits. Numbers denote molar proportion of KCl. Images are photographs taken under reflected light.

30% KCl fluid

Diamond dissolution in 30% KCl fluid produced minimal weight loss. Features generated by 30% KCl fluid (Fig. 3.9) contrasted to those produced in water (Fig. 3.2). Edge dissolution features were dominated strongly by hillocks, which lent a rougher appearance to the diamond than the smooth edges produced in water. A few corners are observed at vertices. (111) faces show similar forms to those produced by H_2O fluid: few, large, flat-bottomed negative trigons and step faces. Face geometry changed from triangular to rounded-triangular, in contrast to the ditrigonal forms produced in H_2O and 5% NaCl aqueous fluid.

60% KCl

Dissolution in 60% KCl fluid resulted in insignificant weight loss. Edge features consisted of hillocks and angular, small corners, although the octahedral form remained largely preserved (Fig. 3.10). Many medium-sized negative, flat-bottomed trigons formed on (111) faces. A few hexagons were also observed. A few trigons penetrate somewhat deeply beneath the diamond's surface. A thin film of graphite appeared on most of the diamond's surface. This style of graphitization and the angular corners are typical for experiments in which fluid escaped the capsule late in the run (Fedorthcouk, personal communication). Therefore the results of this experiment should be interpreted cautiously.

KCl melt

Molten KCl produced little to no vertex- or edge-specific features (Fig. 3.11), and resulted in no significant weight loss. In fact, the measured weight change was actually positive, indicating that this measurement is inaccurate. Edges and vertices did develop a slightly frosty appearance when observed by optical microscopy. The most pronounced features present were

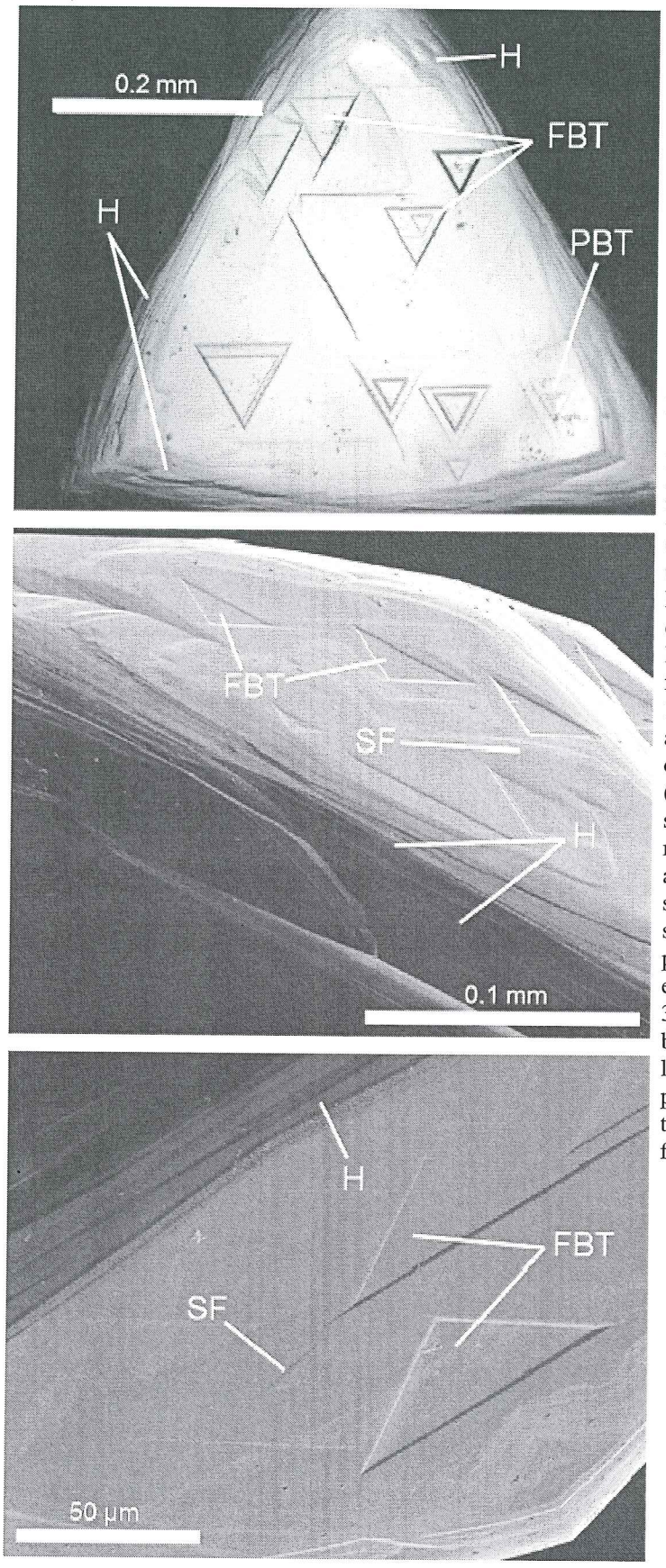

Figure 3.9: Oxidation by 30% KCl-70% H_2O fluid produces step faces, hillocks on diamond edges and large trigons on faces. Diamonds were exposed to 30% KCl-70% H_2O fluid for 60 minutes at 1350 °C and 1 GPa and imaged using optical photography (upper) and scanning electron microscopy (middle and lower). Images shown represent surface features produced in one experiment (run PC-34). FBT: flat-bottomed trigon. H: long hillocks. PBT: point-bottomed trigon. SF: step face.

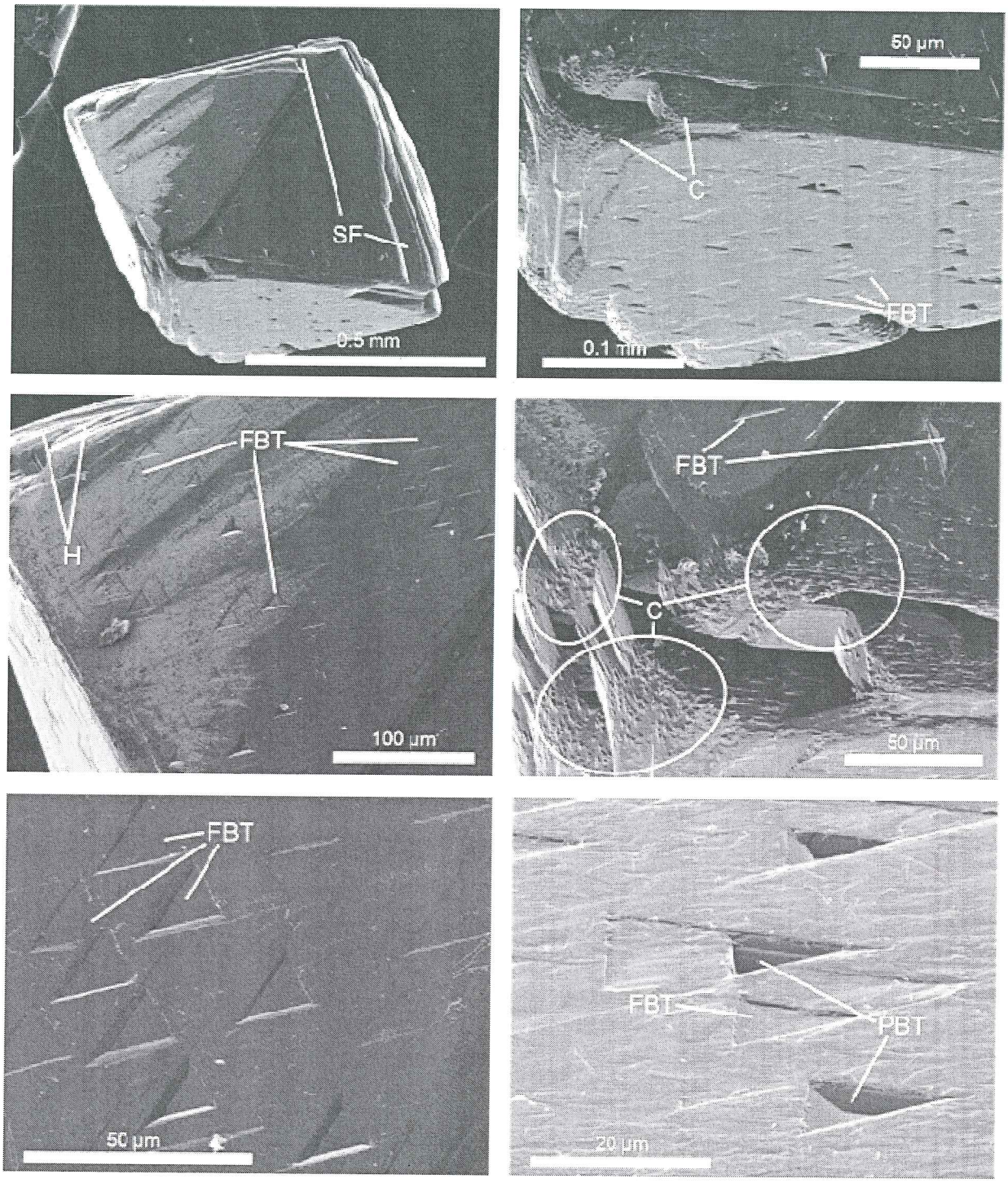

Figure 3.10: Diamond surface after dissolution in 60% KCl aqueous fluid for 60 minutes at 1350 °C and 1 GPa. Medium-sized flat-bottomed trigons appear on (111) faces. Hillocks occur on edges and vertices. Step faces are also present. Small, sharp corners stick out of smoothed vertices, and a thin film of graphite appears as squiggly lines on the surface (lower panels). The corners and graphite film are indicative of late fluid loss (Fedortchouk, personal communication). Diamond was imaged by scanning electron microscopy. Representative results from one experiment (run PC-48). C: corners. FBT: flat-bottomed trigons. H: hillocks. PBT: point-bottomed trigons. SF: step faces.

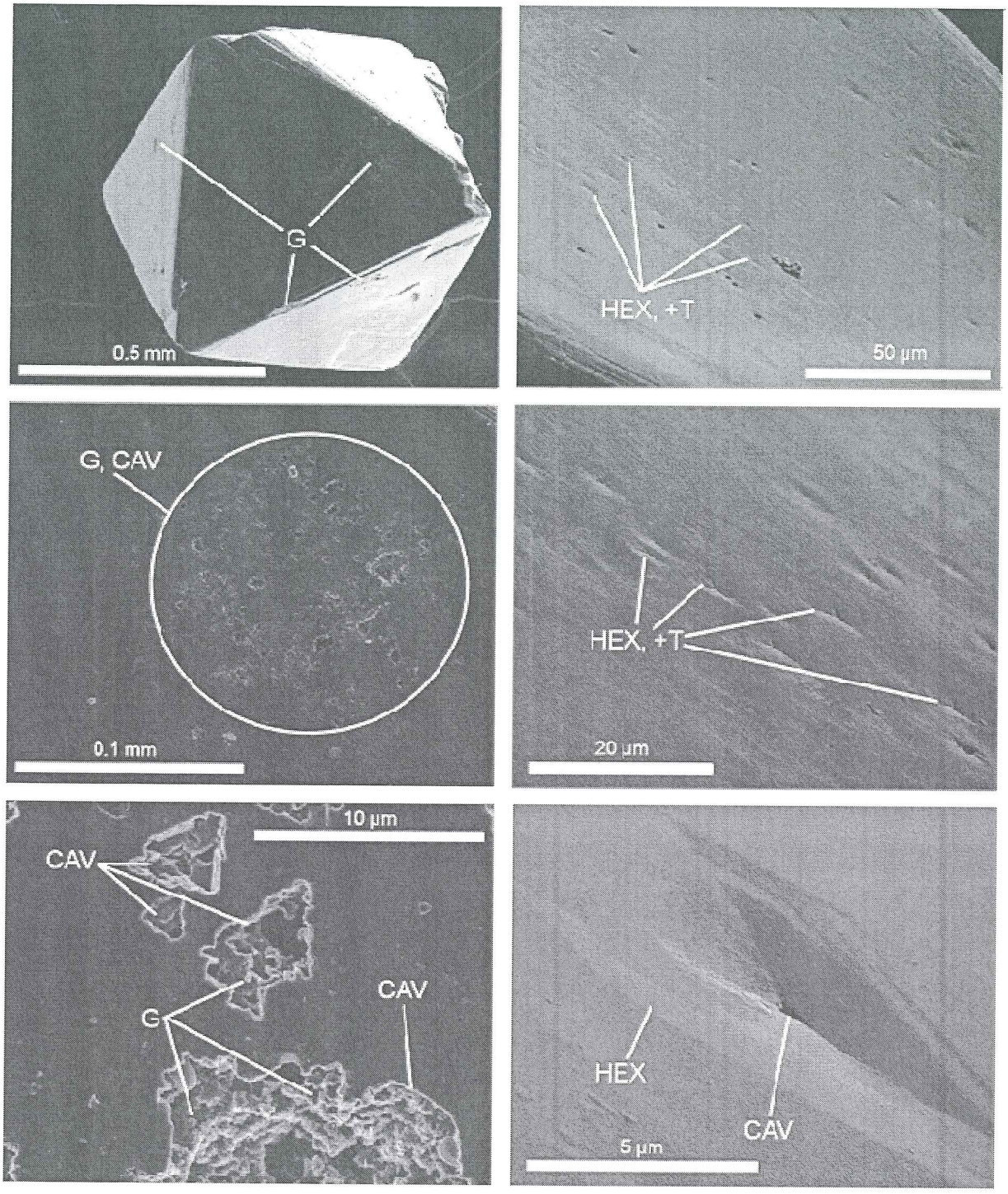

Figure 3.11: Diamond surface after dissolution in KCl melt for 56 minutes at 1350 °C and 1 GPa. Concentrations of irregular cavities are associated with graphitization in rounded areas on diamond surfaces. Hexagons and positive trigons occur on non-graphitized (111) faces. Deep cavities sometimes occur in the vertices and edges of hexagons and trigons. Diamond was imaged using scanning electron microscopy. Images shown represent surface features produced in one experiment (run PC-27). +T: positive trigons. CAV: cavities. G: graphite. HEX: hexagons.

rounded areas of complex etching and graphitization (*ca.* 100 μm in diameter), which appear on both edges and faces. Complex cavities tended to have a mainly triangular form with irregular embayments and tended to propagate deeply into the diamond. Other totally irregular cavities are also present. Such irregular cavities have not previously been observed in high pressure experiments, but do resemble cavities produced in 101 kPa experiments CO gas (Fedortchouk and Canil, 2009). Away from graphitized and irregularly etched areas, small positive trigons and hexagons, and randomly distributed cavities are present. Trigons were both point- and flat-bottomed. Trigon and hexagon edges and vertices sometimes extended into the diamond as deep cavities. As mentioned in Section 3.2.2, the occurrence of positive trigons is noteworthy because they are seldom observed on natural diamonds.

Summary

Diamond dissolution in KCl-bearing aqueous fluid produced many hillocks on edges. Edge dissolution was less pronounced in 60% KCl fluid than in 30% KCl fluid. Trigons became smaller as the fraction of KCl was increased. In KCl melt, deep cavities and graphitization were concentrated in rounded areas, while non-graphitized areas featured few, shallow hexagons and positive trigons. Some cavities were randomly distributed where not associated with graphitized areas.

3.2.4 Comparison of diamond dissolution features produced by NaCl-H_2O and KCl-H_2O fluids

In both the NaCl-H_2O and KCl-H_2O systems, a general evolution of diamond dissolution features was observed with increasing chloride salt content. In both systems, addition of salt tended to decrease the amount of edge dissolution while increasing the roughness of the edges.

High salt content tended to favour face-dominated edge features. However, surface features seem to be more sensitive to the addition of NaCl than KCl – at the same molar salt content, KCl-bearing fluid produced features more similar to those produced in water than did NaCl-bearing fluid.

30% NaCl vs. 30% KCl fluids

In 30 mol % salt, surfaces features produced in both systems show significant differences between one another and from surfaces dissolved by H_2O fluid (Figs. 3.3, 3.8, 3.12). Edge and vertex dissolution features are rougher in character compared to water-dissolved features. The dominant edge features produced by 30% KCl fluid were hillocks. Corners were present to a lesser extent. In contrast, 30% NaCl fluid produced hillocks, corners, disks and crater-and-mound structures on edges and vertices. In general, the edge features of produced by dissolution in 30% NaCl fluid appeared more angular than those produced in 30% KCl fluid. Although apparently less edge dissolution affected diamond exposed to 30% NaCl than 30% KCl fluid, it is unclear whether this is a result of fluid composition or the larger size of the diamond. At least some amount of the difference must result from the different grain size.

Differences were also observed on (111) faces. Both conditions produced flat-bottomed trigons, but those produced in 30% KCl fluid were fewer and larger than those produced by 30% NaCl , although there is considerable overlap between trigon sizes and abundances, depending on the face observed. Some small channel-like cavities penetrated deeply into the diamond exposed to 30% NaCl fluid. These features resemble channels observed on natural diamonds. No such features were observed to be generated by 30% KCl fluid.

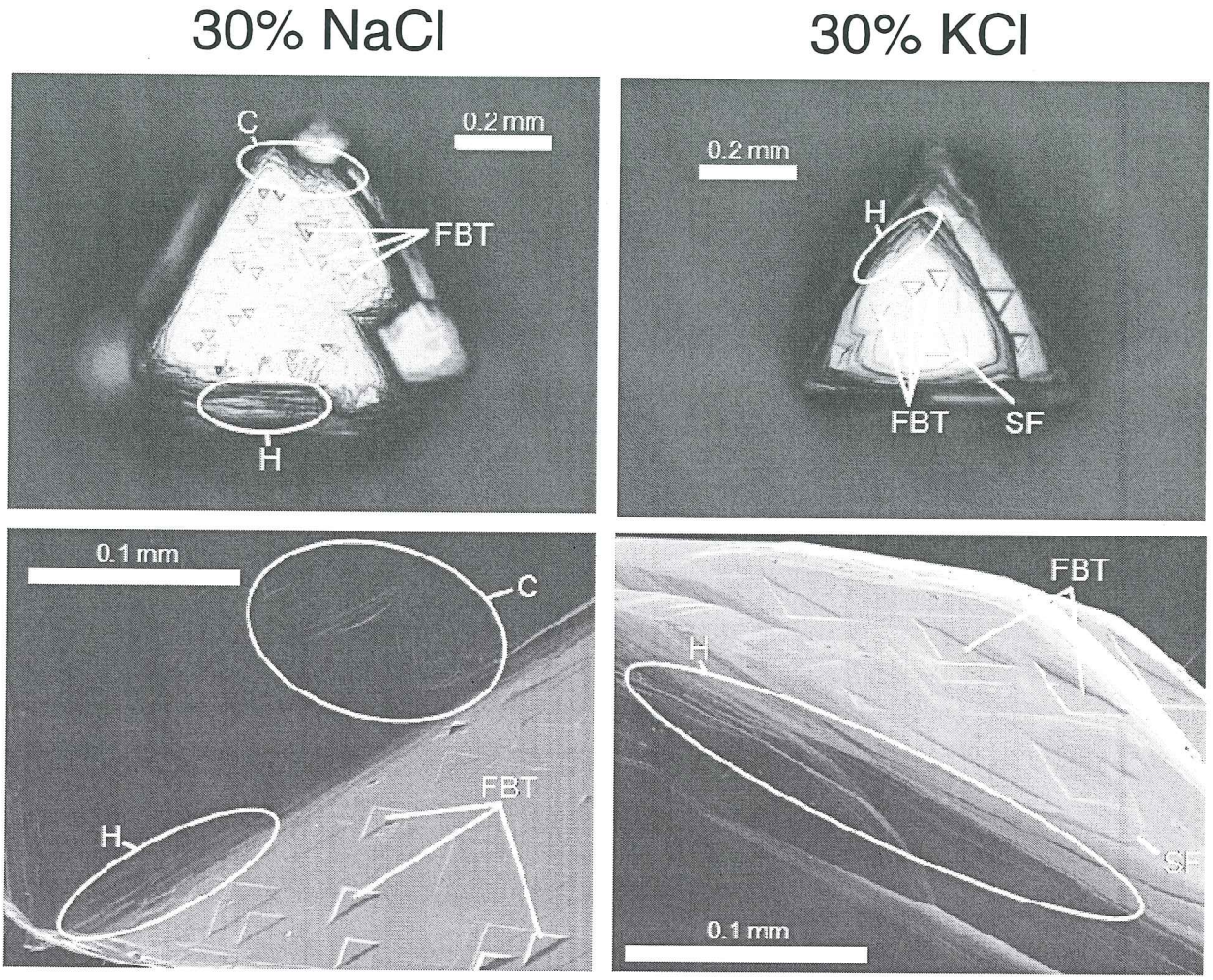

Figure 3.12: Comparison between dissolution features produced in 30% NaCl and KCl aqueous fluid. Edge and vertex features produced by 30% KCl are dominated strongly by hillocks, whereas edges and vertices etched by 30% NaCl consist of corners, hillocks, disks and crater-and-mound structures (the latter two shown in Figure 3.5). Flat-bottomed trigons on octahedrons faces are both smaller and more abundant in the 30% NaCl condition. Complex cavities only appeared on diamond dissolved in 30% NaCl (Fig. 3.5). Diamonds were imaged by reflected light photography (upper images) and scanning electron microscopy (lower images). C: corners. FBT: flat-bottomed trigons. H: hillocks. SF: step faces.

60% NaCl vs. 60% KCl fluids

As for 30% salt compositions, KCl-bearing fluid tended to produce more edge-focused features than NaCl-bearing fluids (Fig. 3.13). Hillocks dominated edges dissolved by 60% KCl fluid, while edges remained largely unaffected in 60% NaCl, featuring few hillocks and corners near vertices. Negative, flat-bottomed trigons were again smaller in 60% NaCl fluid than in 60%

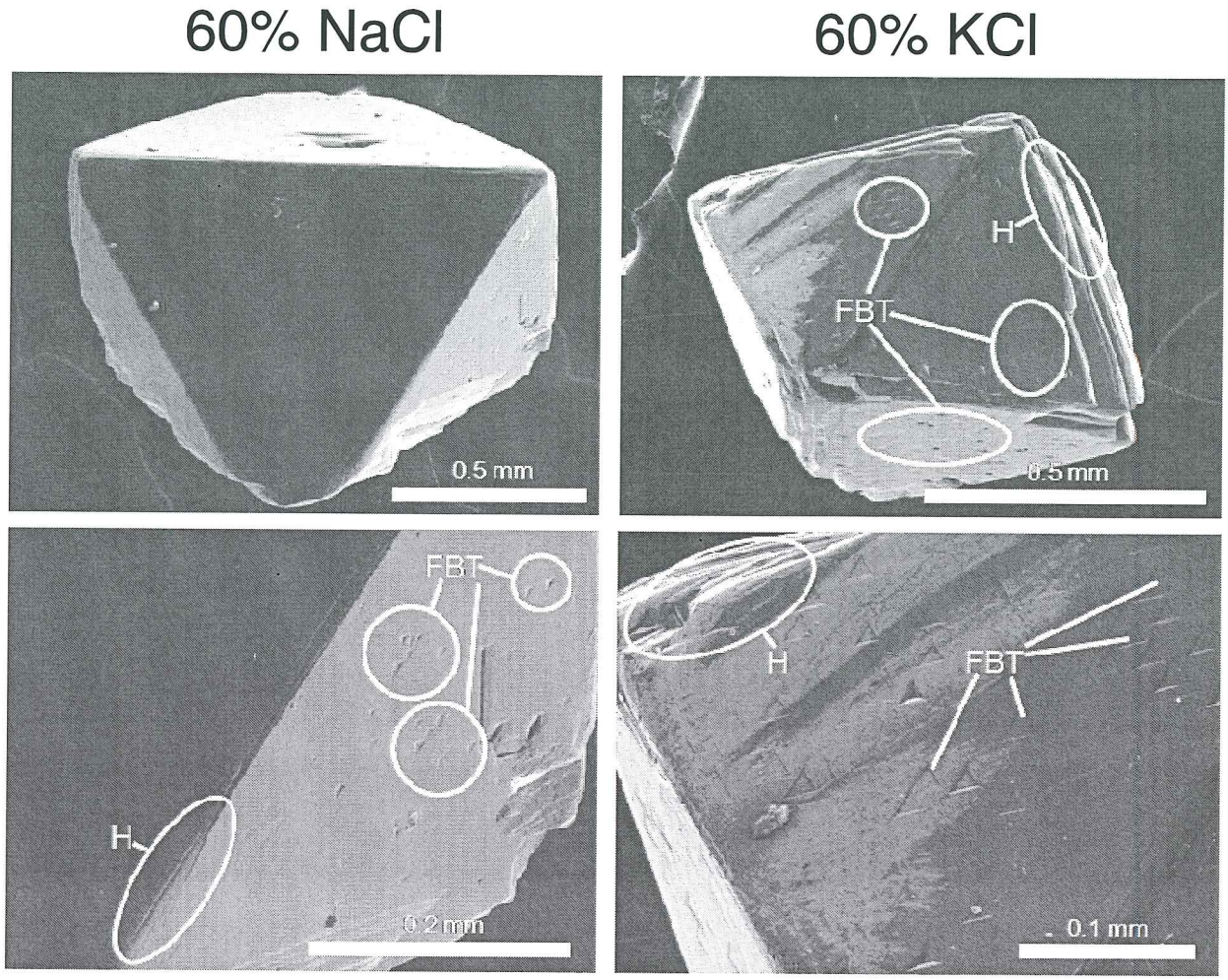

Figure 3.13: Comparison between diamond dissolution features produced by 60% NaCl and KCl aqueous fluids. Both compositions produced abundant, small negative trigons, although trigons produced by 60% KCl were larger. A greater amount of edge dissolution occurred in 60% KCl fluid, resulting in greater expression of hillocks on dissolved edges and step faces. Cavities were only produced in 60% NaCl fluid (Fig. 3.6). FBT: flat-bottomed trigons. H: hillocks.

KCl fluid. Although a few hexagons and more complex cavities were observed in 60% KCl, many more were produced in 60% NaCl. Channel-like cavities were only observed in 60% NaCl. The occurrence of many sharp corners and a thin graphite film in the 60% KCl experiment were likely the result of fluid loss late in the experiment (Section 3.2.3).

NaCl vs. KCl melts

Diamonds exposed to molten chlorides retained their original octahedral shape (Figs. 3.7, 3.11, 3.14). Little to no edge dissolution features were produced. Both salts produced surface graphitization – about half the diamond surface was graphitized in molten NaCl (Figs. 3.7, 3.14), whereas only a small fraction of the surface was graphitized by molten KCl (Figs. 3.11, 3.14). Graphitization was typically confined to rounded areas in both cases. Complex etching was associated with graphitization in both compositions (Figs. 3.7, 3.11, 3.14). Deeply penetrating cavities with were commonly associated with graphitization in molten KCl (Figs. 3.11, 3.14). Dissolution features underlying graphite from the NaCl condition consisted of irregular, relatively shallow forms (Figs. 3.7). Positive trigons were produced on non-graphitized parts of (111) faces in both conditions. Hexagons were observed in the KCl-treated diamond. The density of these etch pits was much greater on the diamond exposed to molten NaCl.

3.2.5 Platinum mobilization in Cl^--H_2O fluids

Spheroidal crystals were observed on diamonds dissolved in 30 and 60% NaCl and molten KCl (Fig. 3.15). Energy dispersive X-ray spectroscopy showed that these spheroids were composed of platinum (data not shown). The presence of platinum spheroids, although a minor occurrence, indicates that platinum was mobilized in these experiments. Although not directly observed in other chloride-bearing compositions, it is likely that platinum was mobilized all of those experiments.

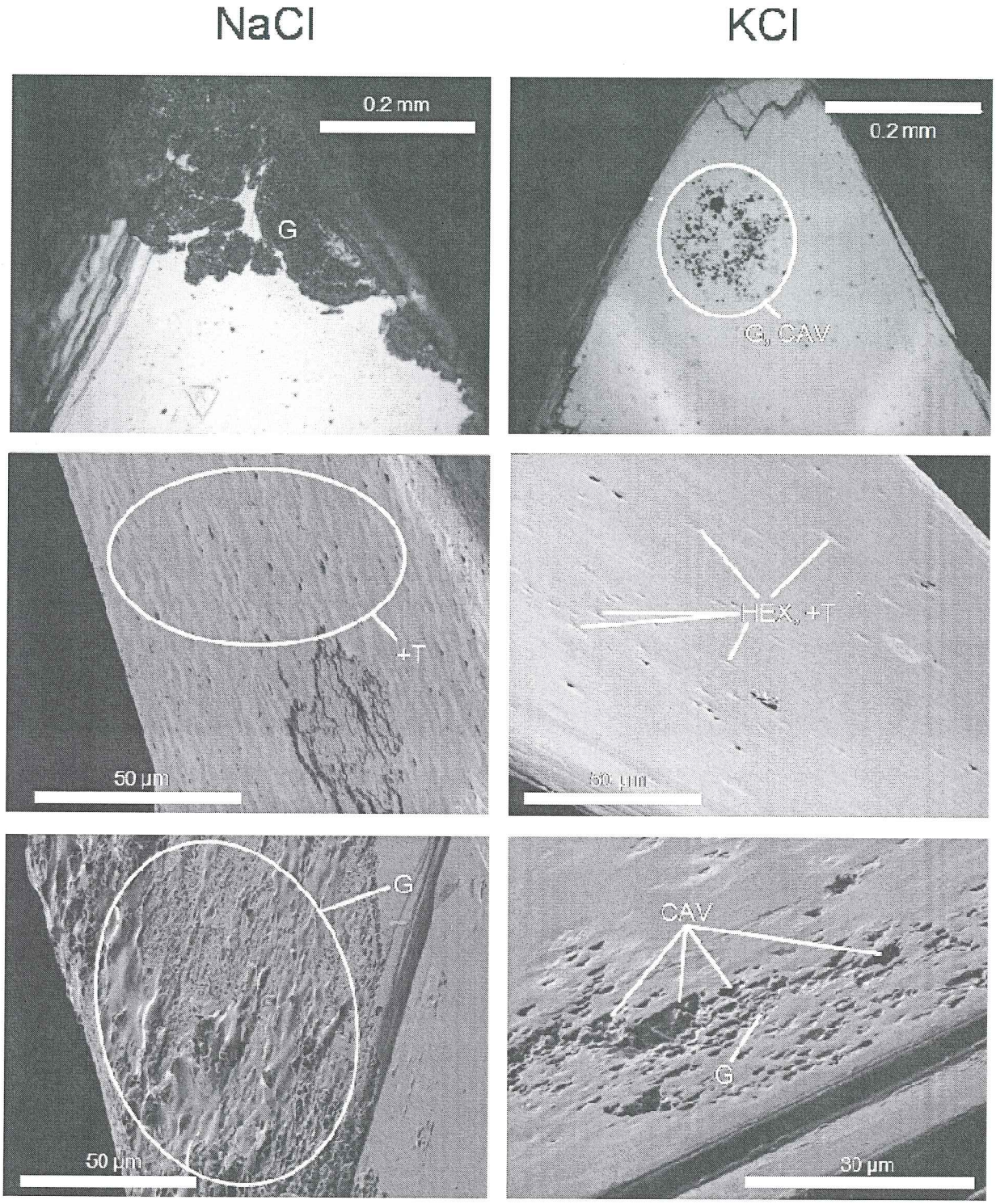

Figure 3.14: Comparison between dissolution features produced in molten NaCl and KCl. Graphitization and associated etching affected diamond under both conditions. The graphitized area was much larger on diamond dissolved in NaCl. Many shallow, point-bottomed positive trigons occur away from graphitized areas on NaCl-treated diamond. Such dissolution pits are less abundant on diamond exposed to KCl melt, and also include hexagons. Diamond exposure to molten NaCl and KCl produces differing intensity of surface forms. +T: positive trigons. CAV: cavities. G: graphite. HEX: hexagons.

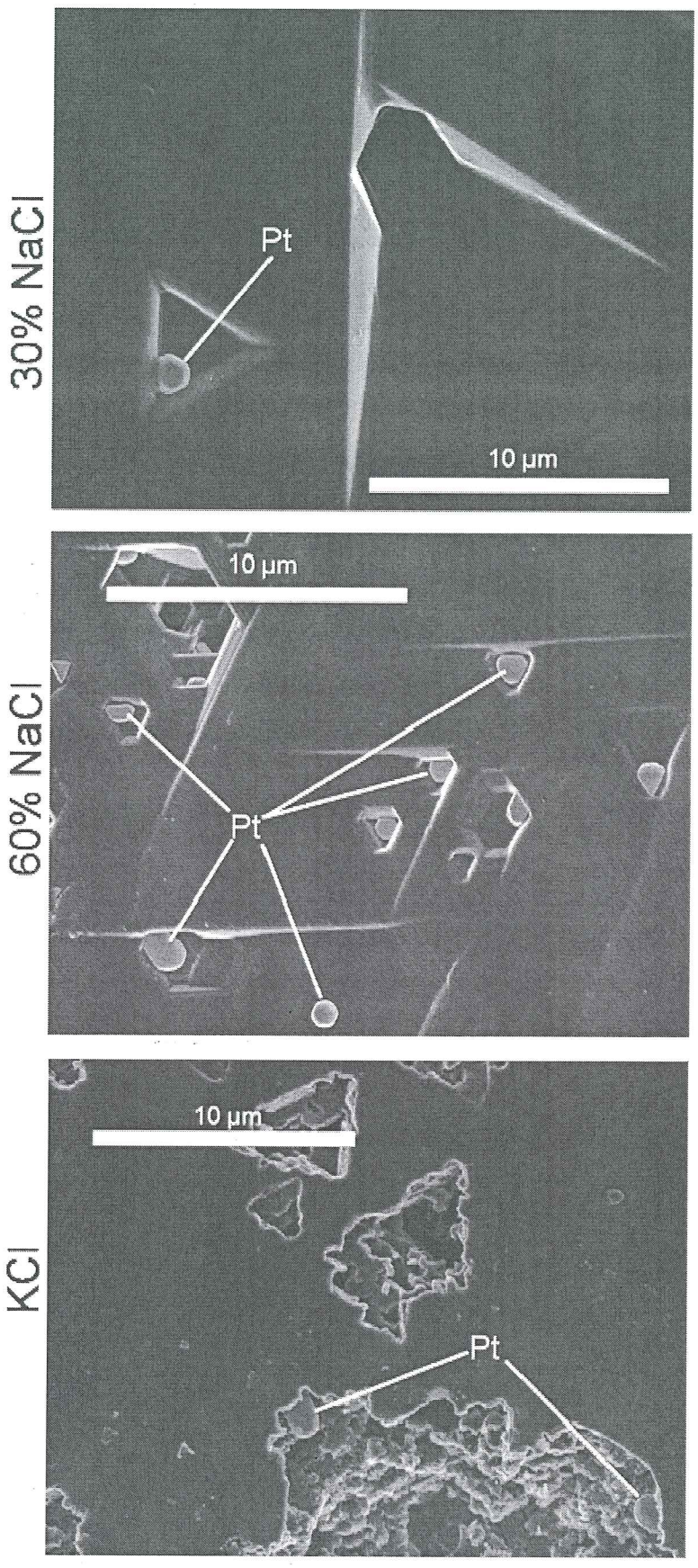

Figure 3.15: Platinum (Pt) spheroids on diamond surfaces after dissolution in 30% and 60% NaCl aqueous fluids and molten KCl. Energy dispersive X-ray spectroscopy confirmed spheroid composition (data not shown). Although such deposits were seldom observed, they indicate that platinum was mobilized during the experiments.

CHAPTER 4: DISCUSSION

4.1 Diamond oxidation mechanisms in Cl^--H_2O systems

4.1.1 Molten chloride-diamond interactions

In order for a chemical to dissolve diamond, it must be able to oxidize carbon from its ground state. Since sodium and potassium are single valance elements, the salts NaCl and KCl should not undergo direct reaction with diamond unless the cations receive electrons from carbon bound in the diamond lattice. This would result in the production of metallic sodium or potassium, which are both extremely reactive metals. In some cases chlorine can also attain positive valences, as in the case of hypochlorite ($[ClO]^-$) and related Cl-O polyatomic anions. However, simple chlorine-carbon compounds, such as CCl_4, contain chlorine as the typical chloride anion. Hence, it is unlikely that there is any direct reaction between NaCl or KCl and diamond.

Invariance of diamond surface features at numerous long duration exposures to molten NaCl at 101 kPa (Fig. 3.1) suggests that no reaction occurred between these components, as expected. Instead, it is most likely that components of air in pore spaces between solid NaCl grains oxidized the diamond during heating. Once the NaCl melted at ~800 °C, it shielded the diamond from further oxidation because volatiles typically have low solubility in ionic melts at low pressure. Indeed, exposure to air for short durations (15 minutes) at the same conditions produced similar forms on diamond. Rudenko *et al* (1979) demonstrated that oxygen, water and CO_2 are the species responsible for diamond oxidation in air at atmospheric pressure.

Contrary to the above predictions, 1 GPa experiments demonstrated that exposure to molten chlorides formed etch pits and graphitization on diamond surfaces (Figs. 3.7, 3.11, 3.14), both of which are attributed to oxidation processes. The rounded shape of graphitized areas on

diamond surfaces shown in this study suggests that fluid bubbles were resting on the surface, interacting with the diamond. This implies that two immiscible fluids were present simultaneously in the capsule with the diamond (Fig. 4.1). Since NaCl and KCl are not known to decompose at the experimental conditions and no other components are intended to be present in the system, we must evaluate the limitations of the method in order to explain the presence of two immiscible fluids in the chloride melt experiments.

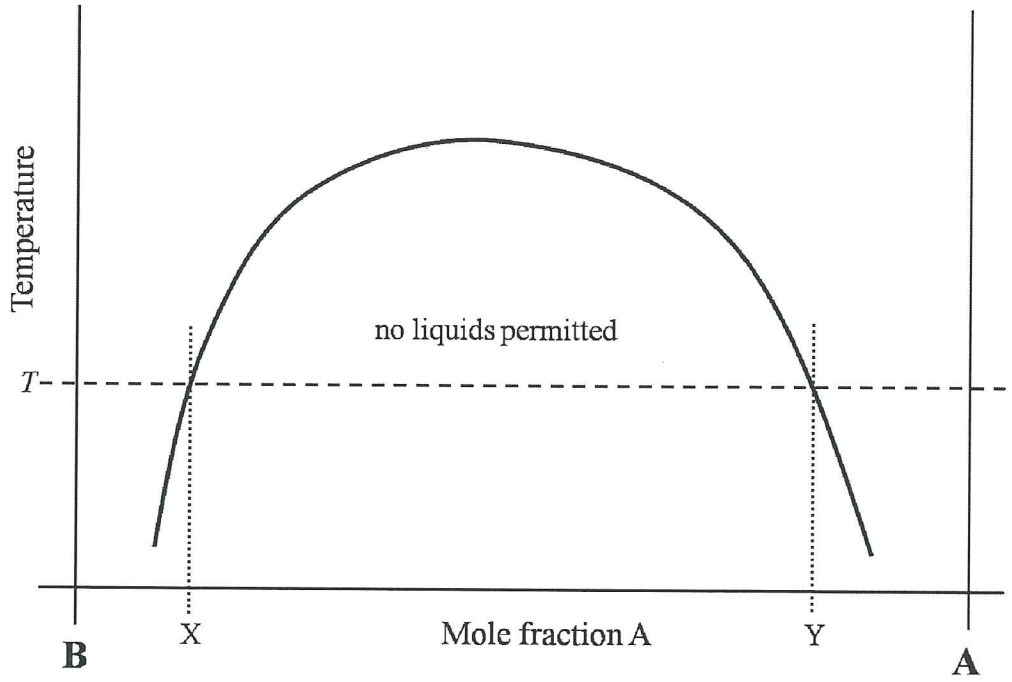

Figure 4.1: Generic liquid immiscibility curve for a binary system (components A and B) at constant pressure. At a constant temperature *T*, no compositions between X and Y can exist as one liquid. Instead they must separate to form two liquids of compositions X and Y, one rich in component B and one in A, respectively. If the two liquids are in equilibrium, each is saturated with the solute (minor) component. If such a system were present in 1 GPa experiments on molten chlorides where component A is the chloride and component B is a fluid impurity, liquid immiscibility could explain the occurrence of rounded areas with abundant dissolution features. Similarly, if component A is kimberlite magma and component B water, a free fluid phase in equilibrium with a kimberlite melt is saturated with kimberlitic solutes.

In all high pressure experiments undertaken in this investigation it is necessarily the case that some amount of air (N_2, O_2, H_2O, CO_2) was sealed inside the capsules during preparation. Furthermore, hydrogen and carbon are known to diffuse freely through platinum at the run

conditions (Luth, 1993). These unwanted impurities may have become dissolved to the limit of saturation in the chloride melt, forming a free fluid phase in equilibrium with the molten salt (Fig. 4.1). Since the volatile impurities should have a low volume compared to the salt melt, and the volumetrically smallest phase should form bubbles in an immiscible fluid mixture, it is likely that the volatile fluid phase was responsible for the rounded graphitized areas observed on diamonds exposed to molten chlorides. The differences observed between dissolution in KCl and NaCl melts could be explained by differing volatile solubility in the different salts or greater volatile activity in NaCl melt than KCl. Since the KCl-dissolved diamond had only small rounded areas of this nature, it would appear that the unwanted volatiles were more soluble in KCl melt. However, if KCl melt had a greater amount of dissolved volatiles, there should have been more etching accomplished by this melt than the NaCl melt. In this regard it would appear that the volatile activity was greater in the NaCl melt. In any case, it is curious that a volatile fluid phase would deposit graphite – previous experiments demonstrated that graphitization occurs in fluid-undersaturated ionic melts at the same run conditions (Kozai and Arima, 2005; Fedortchouk *et al*, 2007), although Evans and Phaal (1961) graphitized diamond in a flow of oxygen at 101 kPa.

Given the similar conditions to Kozai and Arima (2005) and Fedortchouk et al (2007), the chloride melt with dissolved volatiles is a more attractive candidate as the graphitizing agent, but the results suggest otherwise. In order to fully understand this result, it is necessary to characterize the compositions of the two immiscible liquids, which requires additional experiments. Diamond oxidation experiments in the diamond anvil cell would be an appropriate way of addressing this problem. In the diamond anvil cell, a sample is sandwiched between two gem quality diamonds to generate high pressure. Transparency of diamond permits *in situ*

analysis of the sample by spectrophotometric techniques, such as Raman spectroscopy and X-ray diffraction. Raman spectroscopy may be applied to ascertain the components present in the fluids.

Sonin *et al* (2008) reported diamond etching and graphitization by NaCl and NaF melts at 3 GPa and 1300-1350 GPa. They observed negative trigons in contrast to the positive trigons observed in the present study (Figs. 3.7, 3.11, 3.14). They observed graphitization in the longer duration experiments, but did not discuss its morphology or distribution on the diamond surface. It is important to note that the reported diamond weight losses (accurate to ±0.02 mg) do not correlate with experimental durations. Since their experiments also used platinum capsules through which hydrogen and carbon can diffuse (Luth 1993), and air must have been present to some degree in these capsules, there can be no assurance that the features generated were actually produced by interaction of diamond with NaCl and NaF melts, just as is the case in the present study. The absence of a correlation between weight loss and time indicates that the solvent was totally consumed during the experiments. Therefore the solvent could not have been the melt, which was not consumed during experiments, but rather was more likely to have been one or more of the impurity species. Their interpretation that graphitization occurred once the salt became carbon-saturated may be invalid; if the dissolving species was a fluid contaminant, graphitization more likely reflects carbon saturation in that phase, as opposed to the melt. Whether carbon-species saturation is possible in the volatile fluid phase depends on the identity of the fluid, which remains unknown.

4.1.2 The role of defects in determining etch pit sites

It has been suggested that etch pits form where dislocation defects intersect diamond surfaces. According to this mechanism, diamonds showing many etch pits should have higher

dislocation density than those with fewer etch pits. The increased density of etch pits observed on diamonds etched by salt-bearing water compared to water alone clearly indicates that fluid composition is a major determinant of the number of etch pits. However, this observation does not invalidate the importance of crystal defects in determining etch pit sites. Crystal defects are energetically unfavourable compared to normally structured areas, and could therefore determine the most likely locations for dissolution pits, whereas the fluid composition determines the number of pits.

The development of channels may be strongly influenced by dislocations (Lu *et al*, 2001). In order to develop a channel, dissolution must proceed into the diamond. In contrast, dissolution in trigons propagates laterally along the diamond face, increasing the area of trigons as dissolution proceeds. Linear defects could provide an energetically favourable pathway for channel formation. All complex cavities produced in 30 and 60% NaCl fluids were produced within larger trigons (Figs. 3.5, 3.6), and some point-bottomed trigons produced in the KCl condition have deep cavities coincident with their vertices (Fig. 3.11). This coincidence may reflect accelerated dissolution at a dislocation site. It would be interesting to map dislocation outcrops on diamond surfaces prior to conducting dissolution experiments to see whether etch channel sites coincide with dislocations.

4.1.3 Electrostatic attraction in diamond oxidation

Addition of chloride salt to water resulted in a reduction of edge dissolution and an increase in etch pit density on octahedron faces. These correlations may be explained by electrostatic interactions of molecules and ions with diamond surfaces (Fig. 4.2). Any crystal surface is a discontinuity in the crystal structure where open bonds are occupied by surface complexes, such as hydrogen groups bonded to carbon in diamond (Garsuch, personal

communication). At high temperature conditions, there is probably sufficient thermal energy to continually break and reform surface bonds. Since the bonding site density is highest at edges and vertices where (111) planes intersect, and open bonds are electrostatically negative for diamond, it is likely that these locations will preferentially attract electrostatically positive species during bond breaking and reforming events.

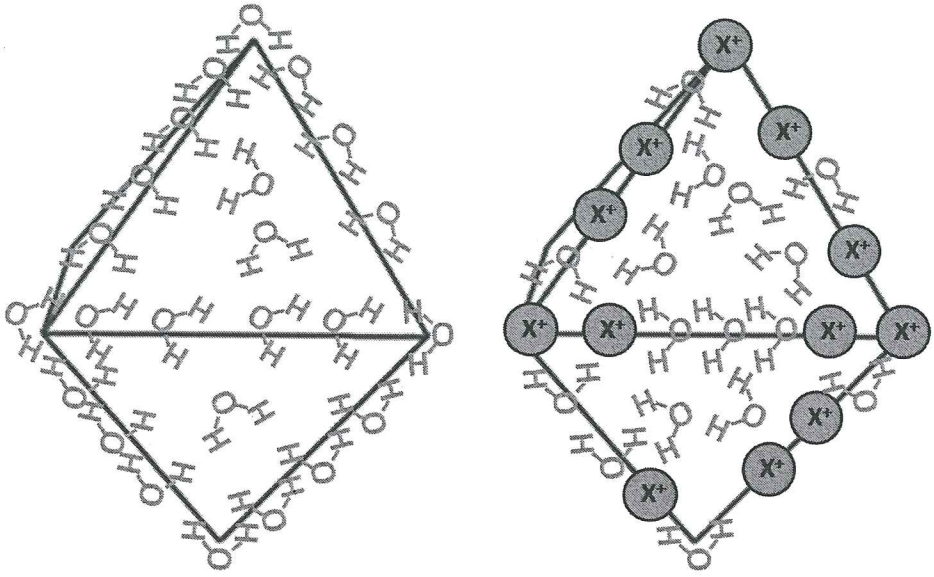

Figure 4.2: Cartoon schematic illustrating the potential role of electrostatic interactions in diamond dissolution. Surface complexes are omitted for simplicity, and as such the illustration can be understood as a representation of the average effect of electrostatic charge. Polar water molecules attract preferentially to more negatively charged edges and vertices, resulting in edge-dominated dissolution features. Introduction of a cation species (X^+) attracts to the more negative sites, blocking water molecules, which are redirected to faces where they produce more trigons.

Consider the case of water, a partially polarized molecule. Where hydrogen surface complexes are present on diamond's surface, the partially anionic oxygen end of the water molecule is likely to react with the hydrogen complexes in an oxidation reaction (Garsuch, personal communication). When the surface complexes are broken, and open bonds are present, it is likely that the partially cationic hydrogen end of the water molecule preferentially reacts with diamond edges and vertices, resulting in the observed rounding of diamond octahedra dissolved in water. When a salt is introduced, the cation species may compete with water

molecules for space at edges and vertices. If the cation cannot change oxidation state, it should not react with diamond (Section 4.1.1). Cations may reduce edge dissolution by blocking the more negatively charged sites on diamond surfaces. This blocking may then increase the likelihood of water molecules binding to the octahedron face, giving rise to more trigons. Indeed, Fedortchouk *et al* (2007) reported less edge dissolution and increased incidence of small trigons on diamonds dissolved in H_2O-oversaturated silicate melt. In this condition, the H_2O fluid should be saturated with ionic solutes from the silicate melt (Fig. 4.1) that may take part in electrostatic blocking.

Previous explanations considered molecular geometries and bond geometries in different directions in the diamond lattice to explain contrasting dissolution forms produced in CO_2 and H_2O fluids (Fedortchouk *et al*, 2007). Here I argue that these differences can equally well be explained by differences in polarity between CO_2 and H_2O molecules. CO_2 is a linear, non-polar molecule and should therefore be more likely to interact with diamond where the bond/charge density is low (*i.e.*, crystal faces). This interpretation is supported by the face-dominated features observed on CO_2-etched diamonds. It is possible that either or both of these mechanisms play a role in diamond oxidation. It would be interesting to undertake diamond dissolution experiments in other polar and non-polar solvents to test this hypothesis.

4.2 Use of diamond surface features as records of chloride content in diamond-dissolving fluids

4.2.1 Distinctive diamond surface features produced by Cl^--H_2O fluids

The dependence of diamond dissolution features on fluid composition has led to the interpretation of diamond surfaces as a proxy for fluid composition (Fedortchouk *et al*, 2008). This study demonstrates that diamond surfaces may preserve a record of chloride-bearing fluids

because surface dissolution forms are dependent on the chloride salt content of aqueous solvent. It is most practical to consider the most distinctive features produced in these compositions for determining fluid composition. At this stage, it is not practical to attempt to determine precise chloride contents by observing diamond surfaces, because there are many other factors that would have to be considered before this would be meaningful, including changes in time, pressure, temperature and oxygen fugacity. Moreover, the dissolution features do not seem adequately sensitive to chloride content to justify precise estimates of chloride content in diamond-dissolving fluids on their basis. However, it is still instructive to evaluate diamond surfaces in the context of this dataset as a semi-quantitative tool for estimating chloride content of diamond-dissolving fluids. Since the salt melt experiments appear to have been strongly influenced by the presence of an unwanted fluid phase (Section 4.1.1), I will consider only the features produced in intermediate fluid compositions below.

Several features produced in chloride-rich compositions were distinctive: (1) high density of flat-bottomed trigons on octahedron faces, (2) low degree of edge dissolution and/or rough edge features, and (3) deep, complex cavities in octahedron faces. These features contrast to those produced in both H_2O and CO_2 fluids. In H_2O, trigons are typically few and well-formed, edge dissolution is pronounced and smooth, and no channels penetrate octahedron faces. In CO_2, trigons are abundant, irregular and cover the entire (111) face, edge dissolution is minimal and no channeling occurs. Natural diamonds having many small trigons, etch channels and rough-edged octahedral form may have experienced dissolution by chloride-rich fluids. Recall however that the diamond dissolved by 30% KCl fluid showed similar trigons to those produced in H_2O fluid and did not exhibit etch channels, and the diamond dissolved in 60% KCl fluid showed only very few channels. On the other hand, the diamonds dissolved in 30 and 60% NaCl

exhibited relatively few edge dissolution features and did have a large number of small, well-formed trigons and a few etch channels. So when interpreting natural diamond surfaces, it is critical to consider that not each of these distinctive features will necessarily be present if chloride-fluid had dissolved the diamond. Furthermore, it is important to note that there are no available data on other H_2O-salt systems at the same conditions as a basis for comparison. Therefore it is not explicitly demonstrated in this study that chloride-borne surface features are distinctive. Other solutes in H_2O fluid may generate similar features. Future experiments could evaluate solutes likely to be in equilibrium with typical kimberlite, such Mg^{2+} and SiO_4^{4-} to evaluate their effects on diamond dissolution features, although the solubility of these particular ions is probably low at the experimental conditions.

4.2.2 Interpreting natural diamond populations

Although certain morphologies and surface features tend to dominate the diamond population from an individual kimberlite pipe, there is a high degree of variability within a population (Gurney *et al*, 2004). Despite that dissolution in CO_2 and H_2O fluids tends to erase previous surfaces features, it is likely that some diamonds retain their surface character established at conditions in the mantle (Fedortchouk, personal communication). Surface feature preservation can be accomplished if some diamonds remain concealed within mantle xenoliths during transport in kimberlite magma. This is likely to be the case because intact mantle xenoliths are a common occurrence in kimberlites. Therefore the significance of diamond surfaces extends beyond deciphering kimberlitic fluid composition and into the realm of mantle fluid compositions.

Fedortchouk *et al* (2008) demonstrated that the Misery kimberlite experienced a late exsolution of free fluid, resulting in highly resorbed diamond morphologies. However, a first

order comparison to surface features produced in the present study reveals broadly similar forms on some diamond surfaces from the Misery population (Fedortchouk, unpublished data). If a detailed comparison confirms the apparent similarities, it would appear that these surface features represent dissolution by chloride-bearing fluid in the mantle. However, 1 GPa experiments simulate a depth of *ca.* 30 km, equivalent to middle or lower continental crust, and it is conceivable that there could be significant differences in diamond surface features produced at higher pressures representative of the upper mantle. Although H_2O- and CO_2-etched diamonds bear broadly similar dissolution features at 1 GPa and 5.7-7.5 GPa (Fedortchouk *et al*, 2007; Khokhryakov and Pal-yanov, 2008), there are notable differences. Furthermore, diamonds graphitize in the presence of carbonate melts at 1 GPa (Kozai and Arima, 2005), but dissolve to form resorption features at 5.7-7.5 GPa (Khokhryakov and Pal'yanov, 2008). The effect of pressure may be significant in Cl^--H_2O fluids as well, and would influence interpretations of diamond surfaces accordingly. It would be interesting to observe diamond dissolution at higher pressure conditions in multi-anvil or diamond anvil cell apparatuses to evaluate the effect of pressure in this system.

In terms of kimberlite fluid composition, the best starting place is to observe diamonds from the Udachnaya-East kimberlite. This kimberlite crystallized magmatic chlorides, as evidenced by immiscibility textures, isotopic analysis and melt inclusions (Section 1.1.2), and hence should have recorded a chloride-rich fluid composition on its diamonds' surfaces, although it is conceivable that the chloride-carbonate magma was low temperature, which would slow the dissolution kinetics. These diamonds should be compared to the results of this study as a means of assessing the applicability of these results to natural diamonds. If Udachnaya-East was anhydrous as originally proposed, the diamonds would be exposed to a dominantly silicate-

carbonate-chloride melt and should show surface features similar to those generated in fluid-undersaturated silicate, carbonate and/or chloride melts (namely graphitization and associated complex etch features). If there was significant H_2O present, Udachnaya-East diamonds should resemble the results shown here for intermediate compositions.

CHAPTER 5: CONCLUSIONS AND FUTURE DIRECTIONS

5.1 Chloride-rich aqueous fluid produces distinctive dissolution features on diamond surfaces

Experiments conducted in this study show that addition of NaCl or KCl to aqueous fluid results in distinctive dissolution features on the surfaces of diamonds at 1350 °C and 1 GPa. Dissolution in water is focussed at diamond edges while saline aqueous fluid produces tends to focus on the (111) face, producing abundant trigons. Edges dissolved in water and low concentration saline are smooth, whereas edges etched in chloride-rich fluids feature a greater proportion of angular hillocks and corners. A small proportion of the etch pits produced in chloride-rich fluid show complex geometries, ranging from polygonal to irregular. Some of these irregular etch pits form deep cavities resembling channels that occur on natural diamonds. Channels have not previously been reported in high pressure studies of diamond dissolution, which may indicate that a high chloride salt content is important in their formation. Etching in KCl-H_2O fluid tends to produce fewer trigons and smoother features than NaCl-H_2O fluid.

It is necessary to repeat these experiments to confirm these findings. In particular, the 60% KCl run must be repeated as it appears to have lost fluid in the late stages of the experiment. Longer duration experiments should be conducted to evaluate the kinetics of dissolution in chloride-rich aqueous fluid. These experiments would also reveal the final morphology of the diamond and the evolution of specific dissolution features. The development of etch channels is especially interesting because they have not been produced experimentally at high pressure prior to this study. Therefore a detailed study of etch channel development may explain their conditions of formation and their occurrence in nature. It is also important to determine if the presence of channels on natural diamonds necessarily requires elevated concentrations of

chloride in the oxidizing fluid.

5.1.1 Diamond surface features: a proxy for chloride content in diamond-dissolving fluids?

Although the results of this study demonstrate that chloride-rich aqueous fluids produce distinctive features on diamonds, there have been no other studies on the effect of other solutes on diamond dissolution. Hence, it is not possible to absolutely conclude that the effect of chloride salts is distinct from that of other solutes, and although other solutes have not been discussed as important components in kimberlitic fluid in the literature, phase relations discussed in Figure 4.1 predict that any fluid in equilibrium with magma must be solute-saturated. There is evidence of variability of dissolution forms among different solutes. Differences exist between features produced in NaCl- and KCl-bearing fluids, and solute-charged water in equilibrium with silicate melt (Fedortchouk *et al*, 2007). Although data are available for H_2O-CO_3^{2-} fluids, they are incomparable to other studies due to the large difference in experimental conditions (> 5 GPa for carbonate studies, 1 GPa in this and other studies). Since CO_2 is often cited as a dominant volatile component in kimberlitic fluid, it is also critical to evaluate the effect of CO_2-Cl^- fluids on diamond dissolution. More data are required before the results of the present study can be applied to natural diamonds as a proxy for unambiguously interpreting diamond surfaces as records of chloride content in dissolving fluids.

Nevertheless, preliminary comparison to diamonds from the Misery kimberlite (Lac de Gras Kimberlite Field, Northwest Territories) suggests that chloride-rich fluid may be a diamond solvent in the mantle (Fedortchouk, unpublished data), but this finding requires confirmation from additional experiments and a more detailed investigation of natural diamond surfaces. In particular, it would be informative to conduct dissolution experiments at pressures of kimberlite origin (*ca.* 6 GPa). If additional evidence supports this conclusion, interpretations that brine

inclusions in diamonds represent diamond-forming fluids must be revised in light of brine-like fluids leaving a dissolution record on diamonds.

5.2 Mechanisms of diamond oxidation

5.2.1 The role of electrostatic attraction in diamond oxidation

Electrostatic interactions are proposed here as an important factor in diamond oxidation. Regions on the diamond surface having a high density of continually breaking surface complexes are ideal locations for reactions involving positively charged species in fluids. Interactions between the diamond surface and polar and cationic constituents of fluid can affect dissolution morphologies and surface features of diamond. Polar oxidizing agents may preferentially dissolve edges and vertices (*e.g.*, H_2O), while non-polar agents may dissolve faces preferentially (*e.g.*, CO_2). Attraction of univalent cations (*e.g.*, K^+, Na^+) to edges and vertices may reduce the amount of edge dissolution produced by a polar species. This mechanism is not in conflict with previous considerations of bonding geometries on the diamond surfaces as a control on preferred dissolution sites of different molecules, as both processes could work in concert. Dissolution experiments using other polar and non-polar solvents could elucidate the role of electrostatic interactions in determining dissolution morphologies and surface features.

5.2.2 The role of crystal defects in determining etch pit sites

Previous studies speculated that dislocation outcrops on diamond surfaces determine where dissolution pits develop. The results of this study clearly show that the number of trigons is dependent on the composition of the solvent, demonstrating that dislocation outcrops do not control the number of dissolution pits. However, the location of dissolution pits most likely coincides with defects on the diamond surface, as these sites are energetically unfavourable and

should dissolve more easily. Deep dissolution cavities within trigons produced mainly in 30 and 60% NaCl fluids support the interpretation that both trigons and channels sometimes develop at dislocation outcrops. This hypothesis could be tested by mapping the defect distribution on the diamond surface and conducting dissolution experiments to see whether there is a relationship between defect sites and the etch pits produced.

REFERENCES

Bohlen, S.R. 1984. Equilibria for precise pressure calibration and a frictionless furnace assembly for the piston-cylinder apparatus. Neues Jahrbuch für Mineralogie, **9**:404-412.

Dunn, T. 1993: The Piston-Cylinder Apparatus. *In* Short Course Handbook on Experiments at High Pressure and Applications to the Earth's Mantle. *Edited by* R.W. Luth, Mineralogical Association of Canada

Evans, T., and Phaal, C. 1961. The kinetics of diamond-oxygen interaction. Pp. 147-153. Conference on Carbon. Pergamon Press.

Fedortchouk, Y., and Canil, D. 2009. Diamond oxidation at atmospheric pressure: development of surface features and the effect of oxygen fugacity. European Journal of Mineralogy, **in press**

Fedortchouk, Y., Canil, D., and Semenets, E. 2007. Mechanisms of diamond oxidation and their hearing on the fluid composition in kimberlite magmas. American Mineralogist, **92**:1200-1212.

Fedortchouk, Y., Matveev, S., Charnell, C., and Carlson, J.A. 2008. Kimberlitic fluid as recorded by dissolving diamonds and crystallizing olivine phenocrysts in five La de Gras kimberlites, Northwest Territories, Canada. 9th International Kimberlite Conference - Scientific Programme and Extended Abstracts,

Francis, D., and Patterson, M. 2009. Kimberlites and aillikites as probes of the continental lithospheric mantle. Lithos, **109**:72-80

Gurney, J.J., Hildebrand, P.R., Carlson, J.A., Fedortchouk, Y., and Dyck, D.R. 2004. The morphological characteristics of diamonds from the Ekati property, Northwest Territories, Canada. Lithos, **77**:21-38.

Izraeli, E.S., Harris, J.W., and Navon, O. 2001. Brine inclusions in diamonds: a new upper mantle fluid. Earth and Planetary Science Letters, **187**:323-332.

Kamenetsky, M.B., Sobolev, A.V., Kamenetsky, V.S., Maas, R., Danyushevsky, L.V., Thomas, R., Pokhilenko, N.P., and Sobolev, N.V. 2004. Kimberlite melts rich in alkali chlorides and carbonates: A potent metasomatic agent in the mantle. Geology, **32**:845-848.

Kamenetsky, V.S., Kamenetsky, M.B., Sharygin, V.V., Faure, K., and Golovin, A.V. 2007. Chloride and carbonate immiscible liquids at the closure of the kimberlite magma evolution (Udachnaya-East kimberlite, Siberia). Chemical Geology, **237**:384-400.

Kamenetsky, V.S., Kamenetsky, M.B., Sobolev, A.V., Golovin, A.V., Demouchy, S., Faure, K., Sharygin, V.V., and Kuzmin, D.V. 2008. Olivine in the Udachnaya-East kimberlite (Yakutia, Russia): Types, compositions and origins. Journal of Petrology, **49**:823-839.

Khokhryakov, A.F., and Pal'yanov, Y.N. 2008: Diamond dissolution forms in water-containing and water-free carbonate melts. 9th International Kimberlite Conference, 1-3.

Klein-BenDavid, O., Izraeli, E.S., Hauri, E., and Navon, O. 2004. Mantle fluid evolution-a tale of one diamond. Lithos, **77**:243-253.

Klein-BenDavid, O., Izraeli, E.S., Hauri, E., and Navon, O. 2007a. Fluid inclusions in diamonds from the Diavik mine, Canada and the evolution of diamond-forming fluids. Geochimica et Cosmochimica Acta, **71**:723-744.

Klein-BenDavid, O., Wirth, R., and Navon, O. 2007b. Micrometer-scale cavities in fibrous and cloudy diamonds - A glance into diamond dissolution events. Earth and Planetary Science Letters, **264**:89-103.

Kozai, Y., and Arima, M. 2005. Experimental study on diamond dissolution in kimberlitic and lamproitic melts at 1300-1420 C and 1 GPa with controlled oxygen partial pressure. American Mineralogist, **90**:1759-1766.

Lu, T., Shigley, J.E., Koivula, J.I., and Reinitz, I.M. 2001. Observation of etch channels in several natural diamonds. Diamond and Related Materials, **10**:68-75.

Luth, R.W. 1993: Apparatus and Techniques for Experiments at Mantle Pressures. *In* Short Course Handbook on Experiments at High Pressure and Applications to the Earth's Mantle. *Edited by* R.W. Luth, Mineralogical Association of Canada

Maas, R., Kamenetsky, M.B., Sobolev, A.V., Kamenetsky, V., S., and Sobolev, N.V. 2005. Sr, Nd, and Pb isotope evidence for a mantle origin of alkali chlorides and carbonates in the Udachnaya kimberlite, Siberia. Geology, **33**:549-552.

Matveev, S., and Stachel, T. 2007. FTIR spectroscopy of OH in olivine: A new tool in kimberlite exploration. Geochimica Et Cosmochimica Acta, **71**:5528-5543.

McDade, P., Wood, B.J., VanWestrenen, W., Brooker, R., Gudmundsson, G., Soulard, H., Najorka, J., and Blundy, J. 2002. Pressure corrections for a selection of piston-cylinder cell assemblies. Mineralogical Magazine, **66**:1021-1028.

Mitchell, R.H. 1986. Kimberlites: Mineralogy, Geochemistry and Petrology. Plenum Press, New York.

Mitchell, R.H. 1996: The Orangeite Clan. *In* Undersaturated Alkaline Rocks: Mineralogy, Petrogenesis, and Economic Potential. *Edited by* R.H. Mitchell, Mineralogical Association of Canada

Mitchell, R.H. 2008. Petrology of hypabyssal kimberlites: Relevance to primary magma compositions. Journal of Volcanology and Geothermal Research, **174**:1-8.

Rudenko, A.P., Kulakova, I.I., and Shturman, V.L. 1979. Oxidation of natural diamond. Novye Dannye o Mineralogii SSSR:105-125.

Safonov, O.G., Perchuk, L.L., and Litvin, Y.A. 2007. Melting relations in the chloride-carbonate-silicate systems at high pressure and the model for formation of alkalic diamond-forming liquid in the upper mantle. Earth and Planetary Science Letters, **253**:112-128.

Scott-Smith, B.H. 1996: Kimberlites. *In* Undersaturated Alkaline Rocks: Mineralogy, Petrogenesis, and Economic Potential. *Edited by* R.H. Mitchell, Mineralogical Association of Canada, pp.

Scott-Smith, B.H., Nowicki, T.E., Russel, J.K., Webb, K.J., C.M., H., M., H., and Mitchell, R.H. 2008: Kimberlites: Descriptive geological nomenclature and classification. 9th International Kimberlite Conference, 1-3.

Sonin, V.M., Zhimulev, E.I., Chepurov, A.I., and Fedorov, I.I. 2008. Diamond stability in NaCl and NaF melts at high pressure. Doklady Earth Sciences, **420**:231-233.

Tolansky, S. 1968. Graphitized natural diamond. Diamond Research:8-10.

Tomlinson, E.L., Jones, A.P., and Harris, J.W. 2006. Co-existing fluid and silicate inclusions in mantle diamond. Earth and Planetary Science Letters, **250**:581-595.

Watson, E.B., Wark, D.A., Price, J.D., and Van Orman, J.A. 2002. Mapping the thermal structure of solid-media pressure assemblies. Contributions to Mineralogy and Petrology, **142**:332-336.